

5-1-2013

Predicting the Performance of a Solar Domestic Water Heating System with Evacuated Tube Collectors and Hydronic Radiant Flooring

Kimberly Nicole Hammer
University of Nevada, Las Vegas, hammerk4@unlv.nevada.edu

Follow this and additional works at: <https://digitalscholarship.unlv.edu/thesesdissertations>



Part of the [Energy Systems Commons](#), [Oil, Gas, and Energy Commons](#), and the [Sustainability Commons](#)

Repository Citation

Hammer, Kimberly Nicole, "Predicting the Performance of a Solar Domestic Water Heating System with Evacuated Tube Collectors and Hydronic Radiant Flooring" (2013). *UNLV Theses, Dissertations, Professional Papers, and Capstones*. 1833.

<https://digitalscholarship.unlv.edu/thesesdissertations/1833>

This Thesis is protected by copyright and/or related rights. It has been brought to you by Digital Scholarship@UNLV with permission from the rights-holder(s). You are free to use this Thesis in any way that is permitted by the copyright and related rights legislation that applies to your use. For other uses you need to obtain permission from the rights-holder(s) directly, unless additional rights are indicated by a Creative Commons license in the record and/or on the work itself.

This Thesis has been accepted for inclusion in UNLV Theses, Dissertations, Professional Papers, and Capstones by an authorized administrator of Digital Scholarship@UNLV. For more information, please contact digitalscholarship@unlv.edu.

PREDICTING THE PERFORMANCE OF A SOLAR DOMESTIC WATER HEATING
SYSTEM WITH EVACUATED TUBE COLLECTORS AND
HYDRONIC RADIANT FLOORING

By

Kimberly Hammer

Bachelor of Science in Mechanical Engineering
University of Nevada, Las Vegas
2010

A thesis submitted in partial fulfillment
of the requirements for the

Master of Science in Mechanical Engineering

Department of Mechanical Engineering
Howard R. Hughes College of Engineering
The Graduate College

University of Nevada, Las Vegas
May 2013

Copyright by Kimberly Hammer, 2013

All Rights Reserved



THE GRADUATE COLLEGE

We recommend the thesis prepared under our supervision by

Kimberly Hammer

entitled

Predicting the Performance of a Solar Domestic Water Heating System with Evacuated Tube Collectors and Hydronic Radiant Flooring

be accepted in partial fulfillment of the requirements for the degree of

Master of Science in Mechanical Engineering

Department of Mechanical Engineering

Robert Boehm, Ph.D., Committee Chair

Yitung Chen, Ph.D., Committee Member

Woosoon Yim, Ph.D., Committee Member

Yahia Baghzouz, Ph.D., Graduate College Representative

Tom Piechota, Ph.D., Interim Vice President for Research &
Dean of the Graduate College

May 2013

ABSTRACT

Predicting the Performance of a Solar Domestic Water Heating System with Evacuated Tube Collectors and Hydronic Radiant Flooring

by

Kimberly Hammer

Dr. Robert Boehm, Examination Committee Chair
Distinguished Professor of Mechanical Engineering
University of Nevada, Las Vegas

Residential solar thermal system installations have been significantly increasing in the last decade and there exists limited resources for reasonably predicting the performance of those systems. A simulated model is developed in MATLAB[®] and used to predict the performance of a solar domestic water heating system. In the simulated system, hot water is generated using evacuated tube solar collectors and stored in a domestic hot water storage tank, which utilizes immersed coil heat exchangers. The system is designed to provide hydronic radiant floor heating to its occupants based on the heat loss of a building energy model for an energy-efficient home. Performance characteristics of the components from well-known manufacturers are utilized where available. Some of the parameters are easily changeable so that several manufacturers' characteristics could be compared using the model. The system's sensitivity to tank thermal stratification and tank size are investigated. For solar intermittencies, the energy required for auxiliary domestic water heating is determined by the model as well. Some empirical investigations of two sets of evacuated tube collectors were used to compare the validity of the model. Results are presented in terms of temperatures and heat gains.

ACKNOWLEDGEMENTS

It is important to me that I first acknowledge Dr. Robert Boehm. Enough cannot be said about the support he has provided me throughout my many years at the University of Nevada, Las Vegas. First as my supervisor in undergraduate research, he sparked the flame for me in solar energy research and continues to provide that motivation today. Then as a professor, he taught me undergraduate heat transfer, introduction to solar and renewable energy, design of thermal systems, graduate thermodynamics, thermal radiation, and ultimately computational solar energy. The final class listed was absolutely essential, if not the driving force, for the simulation within this thesis. Dr. Boehm, through his leadership of the Center for Energy Research, also provided the funding necessary to complete both my undergraduate and graduate degree while gaining hands-on experience at the forefront of solar technology. There were also friendships forged with other students that will undoubtedly last a lifetime. The Center for Energy Research has been my home for many years and I cannot thank Dr. Boehm enough for that initial opportunity.

Another sincere acknowledgement is in order for Rick Hurt, a research engineer at the Center for Energy Research. His guidance, support and previous experiences in thermal engineering were a constant source of reliable knowledge. Also, he allowed for the experimental portion of this thesis to be relatively painless and I'm thankful for that. Lastly, I think it is safe now to concede that his persistent heckling encouraged me to finally complete the research.

The members of my thesis committee also deserve my deepest gratitude. Dr. Yitung Chen was a constant source of encouragement and motivation for both my thesis

and for my academic career. He challenged me continually in engineering and taught me what it truly meant to work fiercely toward my goals. The work ethic I derived from his classes surely played a part in helping me complete this work. Dr. Yahia Baghzouz was a valuable member of the committee and I'm appreciative of his time and insights during the project. I'm also thankful for Dr. Woosoon Yim for managing my final committee member position in the absence of a previous committee member. His support in the final stretch was vital and unwavering.

Lastly, I cannot forget my loved ones. I know they missed me on holidays, birthdays, family trips and special occasions. I think they know I did my best and they continue to encourage me toward my dreams despite my absences. A very special place in my heart will always be reserved for my beagle, Dixie, who fought cancer during the last year of my thesis. She taught me how to be strong and soldier on through it all, and still manage to be friendly towards others. She was an incredible friend and family member, and she will always remind me to value each and every moment with those that I love. I'm so thankful for all the wonderful moments she shared with me, which always left me wanting just one more.

DEDICATION

To Andrew Joseph Wickersham

You believed in me when I was in doubt,

You struggled along side me throughout,

The distance was a lot to weather,

But I love you now, more than ever.

You have earned this dedication.

(Here's to new beginnings...)

TABLE OF CONTENTS

ABSTRACT.....	iii
ACKNOWLEDGEMENTS.....	iv
DEDICATION.....	vi
LIST OF TABLES.....	ix
LIST OF FIGURES.....	x
CHAPTER 1 INTRODUCTION.....	1
1.1 Background.....	1
1.2 Project Motivation.....	3
1.3 Objectives.....	5
1.4 System Components.....	6
1.4.1 System Layout.....	6
1.4.2 Evacuated Tube Collectors.....	7
1.4.3 Dual Coil Heat Exchanger Storage Tank.....	8
1.4.4 Hydronic Radiant Floor Heating System.....	10
1.4.5 Auxiliary and Miscellaneous Components.....	11
1.5 Solar Radiation Fundamentals.....	12
1.5.1 Motion of the Sun Throughout the Year.....	12
1.5.2 System Location.....	14
1.5.3 Solar Irradiance Measurement.....	15
1.5.4 Calculating Solar Angles.....	17
CHAPTER 2 LITERATURE REVIEW.....	22
2.1 Solar Thermal History.....	22
2.2 Previous Analyses.....	22
2.2.1 Evacuated Tube Collectors.....	23
2.2.2 Immersed Coil Heat Exchangers.....	24
2.2.3 Solar Thermal Storage.....	25
2.2.4 Hydronic Radiant Floor Heating.....	27
2.2.5 Solar Thermal System Analysis.....	28
CHAPTER 3 PREDICTING SYSTEM PERFORMANCE.....	30
3.1 Solar Thermal Collector Analysis.....	30
3.1.1 Approximation of Thermal Energy Output.....	31
3.1.2 Hourly Thermal Energy Output.....	35
3.1.2.1 Managing IAM.....	36
3.1.2.2 Collector Efficiency Equation.....	38
3.2 Hydronic Radiant Floor Heating Design.....	38
3.3 Tank Analysis.....	45
3.4 System Calculations Flow Chart.....	49

CHAPTER 4 EXPERIMENTATION.....	50
4.1 Experimental Setup.....	50
4.1.1 First Experimental Setup.....	51
4.1.2 Second Experimental Setup.....	51
CHAPTER 5 RESULTS AND DISCUSSION.....	54
5.1 First Experiment Results.....	54
5.2 Second Experiment Results.....	55
5.3 Simulation Results.....	55
CHAPTER 6 CONCLUSIONS AND RECOMMENDATIONS.....	60
6.1 Conclusions.....	60
6.2 Recommendations.....	61
APPENDICES.....	63
Appendix A Nomenclature.....	63
Appendix B MATLAB Code.....	64
Appendix C Datalogging Program.....	79
Appendix D Component Specifications.....	81
REFERENCES.....	83
VITA.....	87

LIST OF TABLES

Table 1	SolarUs, Inc., SL-30 Tubular Collector Thermal Performance Rating in kWh/panel/day.....	33
Table 2	SolarUs SL-30 transverse incidence angle modifiers.....	37
Table 3	SolarUs SL-30 solar thermal efficiency equation.....	38
Table 4	Domestic hot water draws over a week.....	47
Table 5	Experimental Setup Components.....	53

LIST OF FIGURES

Figure 1	Number of Annual U.S. Solar Installations by Technology.....	3
Figure 2	Annual Installed U.S. Capacity for Solar Heating and Cooling.....	4
Figure 3	System Components Diagram.....	7
Figure 4	[Evacuated Tube] Liquid Heater Designs.....	8
Figure 5	Comparison of air temperatures from floor to ceiling for forced air heating and radiant floor heating.....	10
Figure 6	Solstice and Equinox Days during Earth’s Orbit.....	13
Figure 7	Albedo percentages of some common environmental surfaces.....	15
Figure 8	Beam, diffuse and ground-reflected radiation on a tilted surface.....	16
Figure 9	Pyranometer with shading ring to eliminate beam radiation.....	17
Figure 10	Section of Earth showing β , θ , ϕ , and $\phi - \beta$ for a south-facing surface....	19
Figure 11	The ratio I_d/I as a function of hourly clearness index k_T showing the Orgill and Hollands (1977), Erbs et al. (1982), and Reindl et. al. (1990a) correlations.....	20
Figure 12	Estimated [average] R_b for surface facing the equator as a function of latitude for various $(\phi - \beta)$, by months.....	21
Figure 13	Las Vegas, NV, Solar Radiation for Flat-Plate Collectors Facing South at a Fixed Tilt.....	32
Figure 14	Approximated thermal performance of a SolarUs SL-30 evacuated tube collector tilted at 15 degrees above the latitude for Las Vegas, NV.....	34
Figure 15	Approximated thermal performance of a SolarUs SL-30 evacuated tube collector tilted at various angles above the latitude for Las Vegas, NV.....	35
Figure 16	The planes of the evacuated tube incidence angle modifiers.....	36
Figure 17	The polynomial fit of the relationship between the IAM and the solar incidence angle.....	37
Figure 18	Uponor Joist Trak construction method.....	39
Figure 19	Construction Design Modification of Joist Trak Radiant Flooring.....	40
Figure 20	Modeling Radiant Tube Patterns.....	40
Figure 21	Layout Design Modification of Radiant Floor Tubing.....	41
Figure 22	Summary of Home Floorplan Components and Heat Loss.....	42
Figure 23	System design results from the Uponor Advanced Design Suite for radiant floor design.....	42
Figure 24	Total project heat loss from the Uponor Advanced Design Suite for the radiant floor design.....	43
Figure 25	Home heating and cooling energy load values before and after being filtered for abnormalities in values.....	44
Figure 26	Buderus solar hot water storage tank with dual coil indirect heat exchangers.....	45
Figure 27	Calculation flow chart for the Solar Thermal System simulation.....	49
Figure 28	Experiment 1: SEA Evacuated Tube Collector and Vacuum Tube.....	51
Figure 29	Experiment 2: SolarUS SL-30 Evacuated Tube Collector.....	51
Figure 30	Experiment 2: Pyranometers.....	52

Figure 31	Experiment 2: System components.....	52
Figure 32	Experiment 2: Datalogging equipment.....	53
Figure 33	Averaged hourly thermal output from the SEA 18 Tube Collector.....	54
Figure 34	Averaged hourly thermal output from the SolarUs 30 Tube Collector....	55
Figure 35	100 Gallon Fully-Mixed Tank Temperature throughout the year.....	56
Figure 36	80 Gallon Fully-Mixed Tank Temperature throughout the year.....	57
Figure 37	Two Node, 100 Gallon Stratified Tank Temperature throughout the year.....	58
Figure 38	Two Node, 80 Gallon Stratified Tank Temperature throughout the year.....	58
Figure 39	Two Node, 160 Gallon Stratified Tank Temperature throughout the year.....	59
Figure 40	SolarUs SL-30 SRCC.....	81
Figure 41	Buderus Solar Thermal Storage Tank Specifications.....	82

CHAPTER 1

INTRODUCTION

1.1 Background

As the world's population quadrupled in the last half-century, the demand for energy also severely increased. In order to meet those global energy demands indefinitely, scientists and engineers have been developing and perfecting renewable technologies such as solar and wind energy. Solar energy can be harvested directly in two forms. The first useful form is electricity, which is obtained by exposing a photovoltaic material to sunlight. This technology is generally referred to as *solar photovoltaic*. The second useful form is heat, which is referred to as *solar thermal* technology. In this technology, heat is transferred from sunlight to a working fluid such as oil or water. These technologies are usually at either the industrial or residential scale. At the residential scale, home owners can produce their own hot water from the sun to offset the fluctuations and inflation of gas and electric energy costs. A residential solar water heating system normally consists of the solar collector, the tank used to store the generated hot water, and other components that might be used for auxiliary energy or automated control.

Two typical solar collectors exist for generating hot water: flat plate collectors and evacuated tube collectors. There is a historic debate regarding which technology is more efficient, with evacuated tubes being the newer of the technologies. Because the market for flat plate collectors is much more mature, there exists difficulty in finding unbiased literature. Evacuated tube collectors are sometimes more expensive, but are claimed to produce a larger increase in water temperature from the ambient. They are

also claimed to perform better during cloudy, rainy, windy and sometimes snowy days, depending on the installation [1]. Most resources agree, however, that when designing a solar thermal system that includes space heating, the evacuated tube collector is a better option. Other types of solar collectors, such as the integral-collector storage or batch type, are available but are less common according to the U.S. Energy Information Administration [2]. The solar collector under investigation here is the evacuated tube collector, which has less empirical history than the flat plate collector.

Other components used in conjunction with the evacuated tube collector ensure that the hot water produced is also used optimally. A hot water storage tank is essential for keeping the hot water available for hours outside of solar hot water production, such as after the sun sets. Ideally, solar-produced hot water would be available until the home owners retire for the evening. Even with an optimized hot water storage tank though, solar-produced hot water is not always available. In these cases, an auxiliary component in the system, such as an electric on-demand water heater, may be used to heat the water for residents. A robust system can be strategically designed to the other extreme, where there is intentionally enough hot water to cover space heating loads as well. The system under investigation is designed in this fashion. Hot water used for space heating is typically done in a hydronic radiant floor heating system. Radiant floor heating consists of flexible tubing laid beneath the flooring of the home. Hot water flows through the tubes and conducts heat to the flooring, which then radiates heat to the indoor space and reduces the overall heating load in the winter months.

1.2 Project Motivation

Much evidence can be found which indicates increasing consumer interest in residential solar energy. Figure 1 from Larry Sherwood at the Interstate Renewable Energy Council shows the steady increase in installed U.S. solar technology over a recent ten-year period. Specifically, the increase in solar heating and cooling is shown, which includes domestic water and space heating. Furthermore, Fig. 2 shows that of the increase in installed solar heating and cooling technology, the vast majority are in residential applications [3]. With increasing residential demand in various climates, a need has developed for a simple, accurate way for contractors to predict the performance of a solar thermal system containing evacuated tubes, and not just flat-plate collectors. With that prediction, the best collector can be chosen for the application.

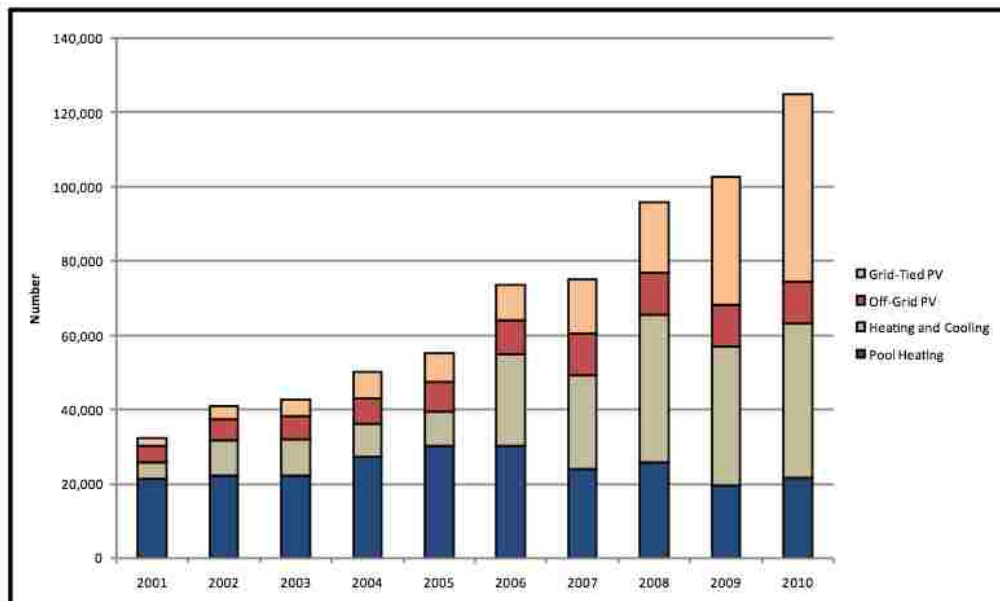
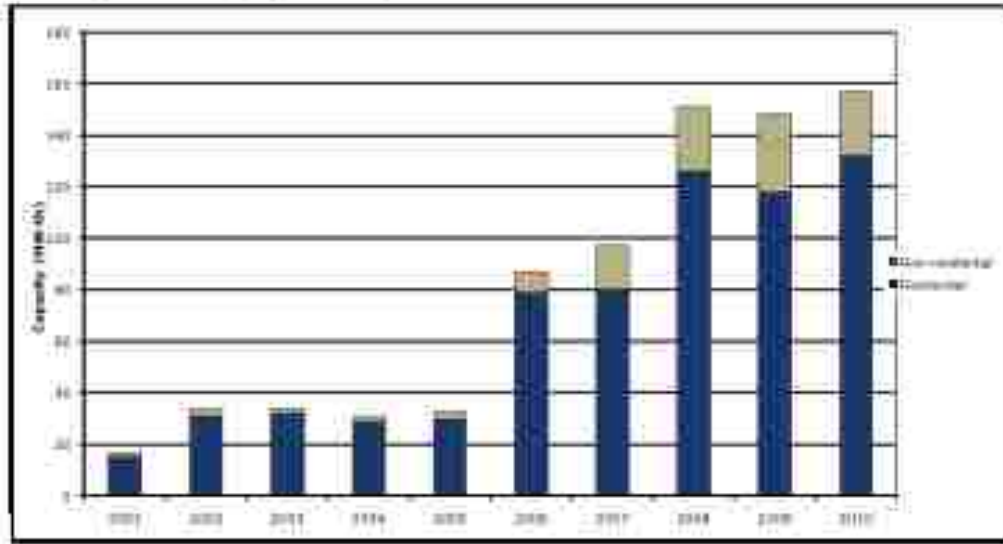


Figure 1. Number of Annual U.S. Solar Installations by Technology (2001-2010). [3]



Based on analysis of software information from ESI and ATSP/CSL.

Figure 2. Annual Installed U.S. Capacity for Solar Heating and Cooling (2001-2010). [3]

Another motivation for developing a simplified model is that predicting the performance of a solar residential hot water system is usually an endeavor left for experienced engineers and solar thermal companies, and it can be daunting for beginning solar engineers and brave homeowners. The performance is sometimes estimated based simply on previous operational experience in the field. At other times, the performance is predicted using computational fluid dynamics software, or TRNSYS[®], and sometimes only focuses on single components because of the complexity, rather than the system as a whole. MATLAB[®] is the scientific programming software used here in an attempt to simplify the simulation of a basic residential system. Many scientists and engineers are familiar with the technical computing software MATLAB[®], which is a benefit for novice programmers. The software is also relatively inexpensive compared to TRNSYS[®] [4], and is readily available at many universities.

1.3 Objectives

The first objective is to create a simplified programming model for the purpose of designing, sizing and evaluating a system's performance for any US location. This programmed model is developed and used in conjunction with an energy-efficient home model. The system's sensitivity to numerous parameters is investigated using the developed model. Some of these investigated parameters are solar collector tilt angle, hot water storage tank size and geographic location. Another parameter of the system is the home energy consumption model, which determines the amount of heating required throughout the year for a home and is done using building energy modeling software. Although this parameter is not tested for sensitivity in the current scope, the model of the solar thermal system is designed to allow for easy substitution if desired in later investigations.

The second major objective is to compare the simulated solar thermal system model with some basic experimental testing. Two experimental setups are used for an initial investigation. The first experimental setup combines a mid-sized evacuated tube collector with a smaller-sized hot water storage tank. In this setup, the water flows through the solar collector and directly into the hot water storage tank, where it would be used for its residential application. The second experimental setup includes a large evacuated tube collector tilted at various angles from the ground. An apparatus is created to be able to easily adjust the collector's tilt angle and also gather two different solar radiation measurements simultaneously. A storage tank is not used in the second experiment, but the heat from the water is sufficiently convected to the ambient during the testing period. Both experimental setups use water as the heat transfer fluid and the

inlet and outlet temperatures of the water flowing through the collectors is recorded. The pump and flow meter in each experiment ensure consistent and accurate flow rates are recorded throughout the testing period.

In the simulated performance model, an effort is also made to utilize manufacturer specified operating data and characteristics of the components where available. There are three important benefits associated with this effort. The first is that the model can be more accurately represented if the components of the system have already been tested. The second purpose for using manufacturer's data is that often times the recorded performance of components is simpler than the mathematical model of the same components. Lastly, manufacturers of solar thermal components are usually bound by the same certification and testing standards. This provides a unique benefit to the simplified model in that manufacturer's data can easily be interchanged. Ultimately, this allows a system designer to compare different manufacturer's component specifications to determine which is best for their application.

1.4 System Components

1.4.1 System Layout

The overall layout, major components, and water flow direction of the solar thermal system under investigation are shown in the system components diagram, Fig. 3. There are three separate systems within the layout that must be analyzed, two of which are closed systems. The first closed system is the solar loop which acts as the boiler to the hot water storage tank. Water is actively moved through the solar loop with a pump, which operates only when the solar collector heats the water to a temperature higher than

the water already in the tank. The second closed system is for the hydronic radiant flooring loop, which also uses a pump to circulate the hot fluid throughout the house. The final system is for domestic hot water, which is the fluid that fills the tank, is stored, and is then distributed to the occupants directly for bathing and other uses.

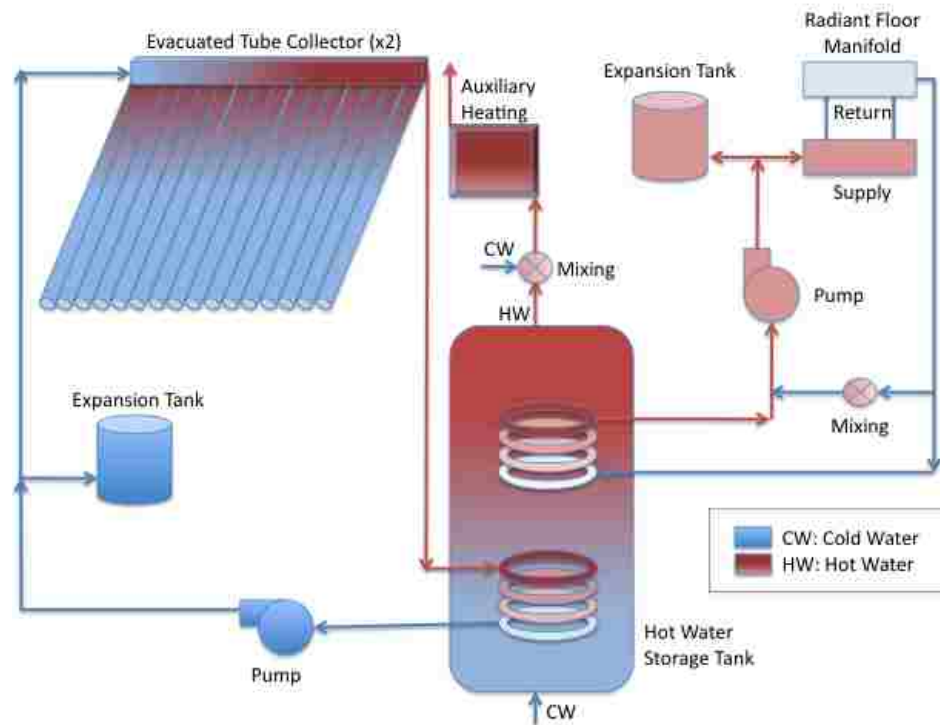


Figure 3. System Components Diagram.

1.4.2 Evacuated Tube Collectors

The solar collector of the domestic hot water system is an evacuated tube collector, which consists of a series of vacuum sealed glass tubes. There are several configurations of vacuum tubes as shown in Fig. 4, but essentially, all have an external glass envelope, an internal absorber plate, and a heat transfer pipe containing fluid [5]. The glass envelope is actually two glass tubes, one within the other, and joined at the exposed end to create a vacuum layer around the central absorber and heat pipe. The

glass tubes are evacuated during manufacturing, which, at its end use, reduces the convective and conductive heat loss from the hot copper tubes to the cool ambient air. The sun's radiation penetrates the vacuum to the copper heat pipe and heats the internal fluid to a boil; which then causes it to rise to the bulb at the top of the tube. The manifold that spans the top of the collector contains and insulates the hot bulbs at the tops of each tube. Water from the solar loop enters the manifold and absorbs the heat from the bulbs in series, where it then exits the manifold as hot water.

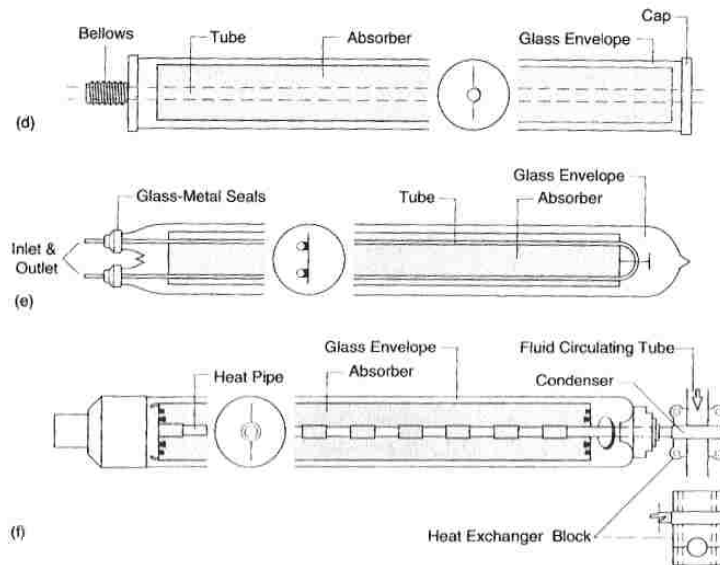


Figure 4. [Evacuated Tube] Liquid Heater Designs. Adapted from [5].

1.4.3 Dual Coil Heat Exchanger Storage Tank

Several different types of tanks exist that are particularly suited for solar hot water storage and these tanks promote different system layouts. Some systems use two smaller tanks rather than one large tank, so that one can be used as a solar preheat tank and the other for domestic storage. Of interest in this investigation is the dual coil, indirectly fired hot water storage tank. This type of tank has two internal heat exchangers in the form of a helical coiled pipe with inlet and outlet connections at the wall of the tank. The internal

heat exchanger is referred to in the literature as an immersed coil heat exchanger or a helical coil heat exchanger. The bottom coil is used for the solar loop so that the optimal heat transfer can occur between the coldest water in the tank and the hot solar fluid. Because of this, the coil outlet that flows to the collector is the lower of the two connections, and the higher is for the coil inlet, where the hot water can be positioned higher in the tank.

The strategy for solar thermal storage is aimed at stratifying the temperatures within the tank. Stratification is an important concept in modeling any hot water storage tank because it changes the way the model is analyzed. If a tank has its coldest water in the bottom, hottest water in the top, and a consistent temperature gradient in between, the tank can then be modeled as a stratified tank with more than one temperature node. The alternative to this is a fully-mixed tank where the temperature is approximated to be the same throughout the fluid. The simulated model of a fully-mixed tank reduces the effective heat transfer from the lower coil because the temperature at the bottom of the tank will no longer be colder than the temperature at the top. With the lower coil heat exchanger effectiveness reduced, the fully-mixed tank model will result in greater solar energy or auxiliary energy need than in a stratified model. Both stratified and fully-mixed storage tank models are considered in the investigation and discussed in the results.

The second closed loop utilizes the upper coil, and the domestic water heating system utilizes the tank itself. The fluid within the tank does not mix with the fluid in the coils. Cold, supply water enters the tank near the bottom to replace the hot water drawn from the top of the tank. These hot water draws are modeled for a seven day period and represent domestic consumption that repeats weekly. The top coil of the tank can be used

for several applications, such as pool heating, but here the top coil is modeled for the loop of the radiant floor space heating.

1.4.4 Hydronic Radiant Floor Heating System

Many types of radiant flooring systems exist, and they can be either hydronic or electric resistance heating. In a hydronic radiant flooring system, tubes are laid beneath the flooring which carry hot water during system's operation in the heating season. The heat from the fluid is conducted to the top most layer of flooring and then radiates to the occupants of the home. This radiant flooring provides the residents the thermal comfort they require for the duration of the heating season. Figure 5 shows that the floor to ceiling temperature gradient is almost ideal for radiant floor heating compared to the severe mismatch of forced air heating. For an energy efficient home, radiant floor heating is ideal for an energy efficient home because the occupants will feel comfortable while consuming less energy throughout the heating season.

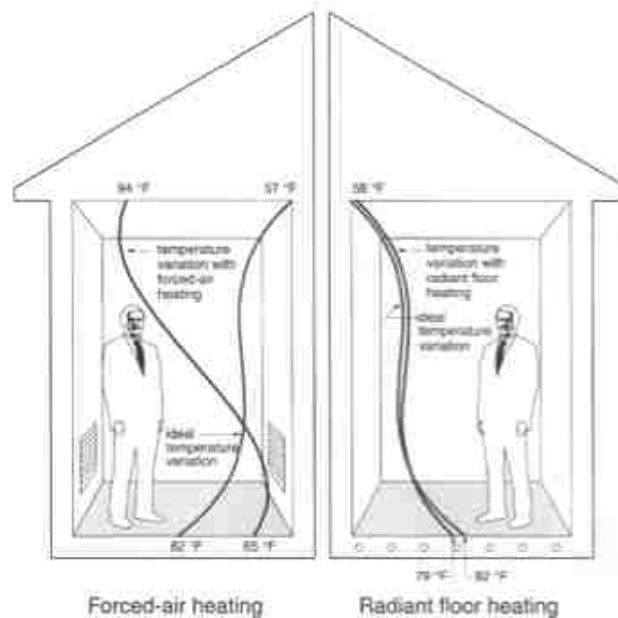


Figure 5. Comparison of air temperatures from floor to ceiling for forced air heating (left), and radiant floor heating (right).

The radiant floor heating system is operational during the heating season only and will provide space heating when hot water is available beyond the domestic water draws. Hot water from the storage tank will flow to the supply manifold where the amount of water needed is distributed through the radiant floor loops. The loops end back at the manifold on the return side where the water can be reheated in the upper coil of the tank. When hot water for radiant flooring is not available, and space heating is still needed, the auxiliary home heating system becomes operational. Similarly, if the water within the tank is not hot enough for domestic use, the auxiliary water heating component in the system will heat the water for residents.

1.4.5 Auxiliary and Miscellaneous Components

Other components are of course necessary to make sure the solar thermal system is safe, functional, and easily maintained. An important safety measure is the use of expansion tanks for containing fluid expansion as it is heated in the system. Not shown in the system layout, but also included in the design is an automatic air vent connected to the solar thermal loop at the highest point in the system to release any air in the liquid. Another safety feature of the design, which prevents scalding from domestic water, is a mixing valve immediately after the hot water exits the top of the tank allowing cold water into the line if needed. With the mixing valve preventing scalding, the tank can be heated above the required domestic water temperature for the storage of more thermal energy. To maintain the relatively low radiant loop temperature, another mixing valve allows for the cooler return water to bypass the solar hot water heat exchanger or to only reheat a fraction of the return water for the next loop iteration. Auxiliary components are required for both back-up water heating of domestic water and also for space heating in the colder

months. Many options are available for auxiliary water heating including natural gas and electric. Since natural gas is still a non-renewable energy resource, although very affordable, the model assumes the auxiliary water heater will be electric. Auxiliary space heating is assumed to be done with a mini-split heat pump, which is also electric in operation. Auxiliary heating could also be provided to the radiant flooring system, but it is not used in this simulated model. Proper valves are essential in any solar thermal system and a significant set of valves allow for the solar and radiant loops to be filled with fluid. Although not shown on the system layout, a ball valve separating two fill and drain valves provides the necessary break in both lines to purge air and fill with fluid.

1.5 Solar Radiation Fundamentals

1.5.1 Motion of the Sun Throughout the Year

The sun is the fuel source for a solar domestic water heating system. Unlike other sources of fuel, the sun's energy cannot be delivered continuously throughout the day, or even the year, because of its diurnal and seasonal nature. An optimized solar energy system will take advantage of those fluctuations. It is therefore important to understand the fundamental nature and motion of the sun in designing a solar thermal system.

During the course of a year, the sun will once reach its highest point in the sky and once reach its lowest point. At its highest point, the day is also the longest of the year and is called the summer solstice. At the sun's lowest point in the sky, the day is the shortest of the year and is called the winter solstice. The date of the summer solstice in the northern hemisphere is June 21st, which is also the winter solstice in the southern hemisphere. This means that on June 21st, the northern hemisphere experiences its longest day and the southern hemisphere will experience its shortest day. And likewise,

December 21st is the winter solstice in the northern hemisphere and summer solstice in the southern hemisphere. There is also a day between each of the solstices where the length of day and night are equal, which is the equinox. The solstices and equinoxes generally coincide with the heating and cooling seasons. Another important consideration regarding heating and cooling in the southern hemisphere is the tilt of the Earth during its orbit around the sun. As shown by Fig. 6, the southern hemisphere is tilted toward the sun during its summer and tilted away from the sun during its winter. The tilt amplifies the heating and cooling seasons in the southern hemisphere and the solar thermal system design should take that into account.

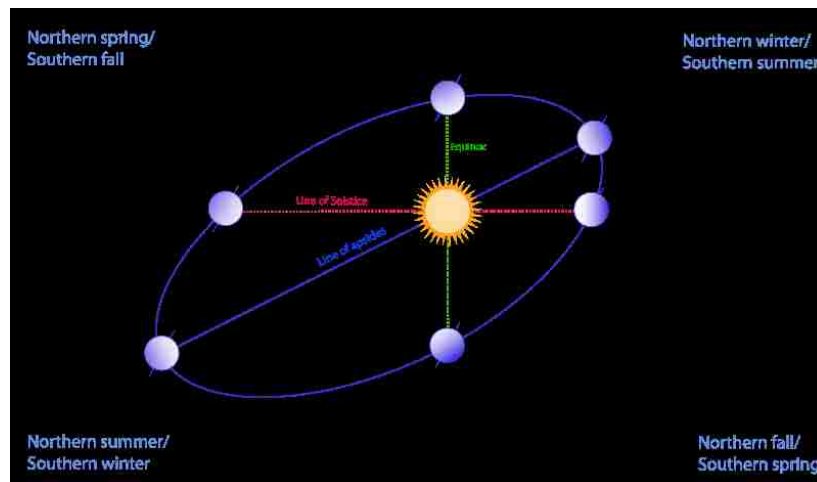


Figure 6. Solstice and Equinox Days during Earth's Orbit. [6]

Since a solar thermal collector gains the most energy when tilted normal to the sun, the tilt angle will determine whether more energy is collected in the winter or the summer. Knowing the extreme angles of the sun throughout the year for a given location, along with the home heating and cooling seasons, a designer can create an optimized system. For example, in the northern hemisphere, a system designed for the heating season should be tilted to collect energy from the average, low, winter sun angle. A

system designed for consistent energy production throughout the year would instead be tilted at the latitude of that location, which coincides approximately with the angle of the sun at the two equinoxes.

1.5.2 System Location

The only way to properly determine the motion of the sun throughout the year is to first determine the latitude and longitude of the location for the system being designed. Other factors regarding location also play an important role in how much energy is available to a solar collector. Climate is one of those important factors, which includes the quantity and frequency of cloud cover, precipitation, and whether freeze protection will be a requirement of the system. Evacuated tube collectors are typically better suited for freeze protection over flat plate collectors because the vacuum within the tubes prevents convective heat loss. Going beyond the climate of the system's location, factors of ground reflectivity and shading are also a concern and should be considered in predicting the performance of solar collectors. Lighter colored surfaces will reflect some of the sun's energy from the ground back to the collector. The ratio of energy incident upon a surface to that reflected from the surface is typically given in the form of an albedo, or reflection coefficient. Typical values of albedo for varying ground surfaces have been previously determined as shown in Fig. 7. The albedo is shown in terms of a percentage which is used as a decimal in determining ground reflected solar radiation. Most environmental conditions that a solar thermal collector will experience are within the albedo range of 0.1 to 0.3.

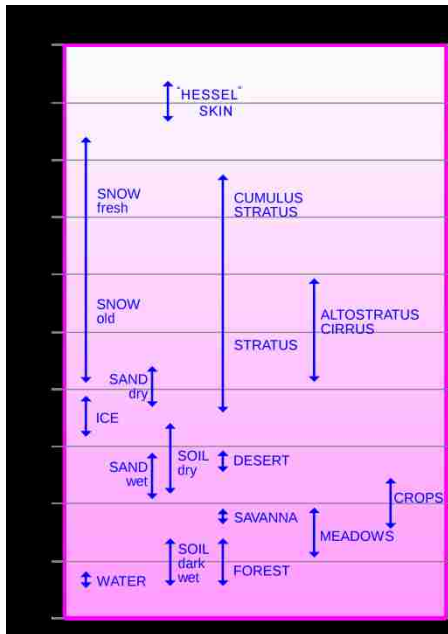


Figure 7. Albedo percentages of some common environmental surfaces. [7]

1.5.3 Solar Irradiance Measurement

Extraterrestrial radiation is the solar energy which is incident on a horizontal surface at the outer atmosphere. As the energy travels into the atmosphere, some of the light is absorbed, reflected and diffused by particles in the air, and by the air molecules themselves. Air pollution, and the system's elevation above or below that pollution, also plays a major role in how much solar energy is available for the collector to absorb. Measurements of solar radiation taken at ground level are therefore lower than the radiation values at the outer atmosphere. Solar irradiance measured at ground level is typically presented in three forms: global horizontal irradiance, direct normal irradiance and diffuse horizontal irradiance. Each of these are in units of power over a unit area.

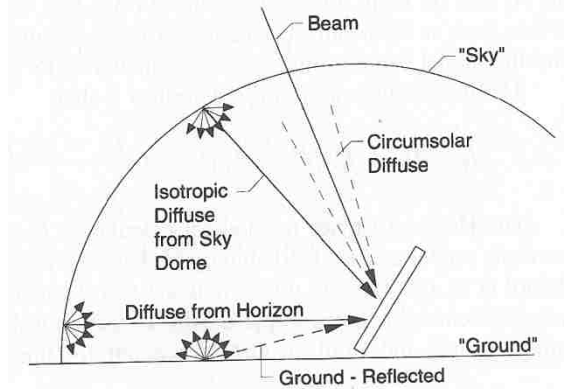


Figure 8. Beam, diffuse and ground-reflected radiation on a tilted surface. [5]

Solar radiation measurements are done with different forms of radiometers depending on the type of solar radiation to be measured. Direct normal irradiance, also called direct or beam radiation as shown in Fig. 8, is the measure of radiation coming directly from the solar disk, which is the type of radiation that causes shadows from objects. A pyrheliometer is pointed normal to the sun and tracks it in both elevation and from east to west throughout the day to record the direct normal irradiance. The viewing window pointed at the sun is small enough to block out radiation from any other sources. Global horizontal irradiance is the measure of radiation coming from the entire sky dome, including both the radiation diffused from air particles and the direct beam coming from the sun. A pyranometer usually rests horizontal on the ground and contains a 180 degree clear glass dome on top to allow all radiation from the horizon and higher to enter the radiometer for measurement. Solar radiation which is not beam radiation is called diffuse radiation. On an overcast day for example, all of the solar radiation will be diffuse which still provides light, but not enough to cause any shadows behind ground objects. A modified pyranometer is capable of measuring only the diffuse component of radiation by blocking out the solar disk continuously throughout the day with either a shadowing ring

shown in Fig. 9, or tracking ball [8]. This pyranometric modification is typically how the final type of solar radiation, diffuse horizontal irradiation, is measured.

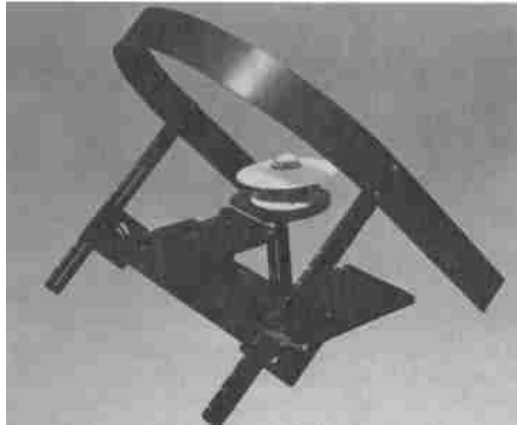


Figure 9. Pyranometer with shading ring to eliminate beam radiation. Courtesy of the Eppley Laboratory. [5]

1.5.4 Calculating Solar Angles

Duffie and Beckman [5] give a thorough analysis of the process of determining the beam, diffuse and reflected components of radiation on both a horizontal and tilted surface. A summary of the analysis is used here to give guidance in following the programmed model in Appendix A. Solar radiation on a tilted surface is usually derived from the horizontal radiation and depends on the tilt angle of the solar collector. The relationships that define the sun's position throughout the days of the year are based in solar time. Solar time is an adjustment from standard local time since they do not coincide. At noon in solar time, the sun is halfway through its path from the east horizon to the west horizon, which is not always the case for local time. The difference in minutes between the solar time and the standard local time is given by

$$\text{Solar time} - \text{standard time} = 4(L_{st} - L_{loc}) + E \quad (1)$$

where L_{st} is the standard meridian in degrees for the local time zone determined by multiplying the hours from local time to Greenwich Mean Time by 15 degrees. L_{loc} is the

longitude in degrees west at the location of the solar thermal system. The last variable, E , accounts for variances in the Earth's rotation and corresponds to the equation of time in minutes given by

$$E = 229.2(0.000075 + 0.001868 \cos B - 0.032077 \sin B - 0.014615 \cos 2B - 0.04089 \sin 2B) \quad (2)$$

where the variable B is determined from Eq. (3) and depends on n , the day number of the year from 1 to 365.

$$B = (n - 1) \frac{360}{365} \quad (3)$$

Knowing the solar time, the angles used in determining the sun's position throughout the year can be determined. The hour angle of the sun, ω , is given by Eq. (4) and the declination angle of the sun, δ , can be determined for any day of the year using Eq. (5). Finally, Eq. (6) gives the zenith angle, θ_z , for the angle between the vertical and the line to the sun where the latitude is represented by ϕ .

$$\omega = -(12 - \text{Solar time}) * 15^\circ \quad (4)$$

$$\delta = 23.45 \sin \left(360 \frac{284 + n}{365} \right) \quad (5)$$

$$\cos \theta_z = \cos \phi \cos \delta \cos \omega + \sin \phi \sin \delta \quad (6)$$

Other important angles that define the solar collector's orientation are also needed to find the amount of incident solar radiation available. The first is the slope, β , which is the tilt of the panel from the horizontal with 90 degrees being vertical as shown in Fig. 10.

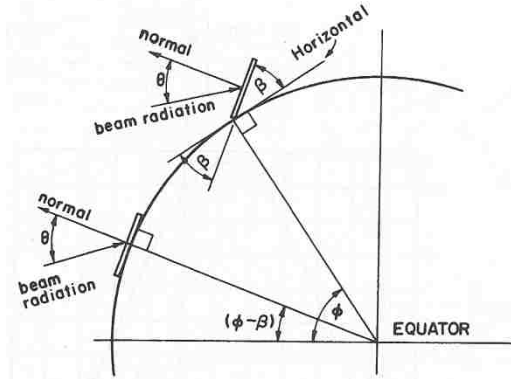


Figure 10. Section of Earth showing β , θ , ϕ , and $\phi - \beta$ for a south-facing surface. [5]

Another important angle is the azimuth angle, γ , which corresponds to the solar collector's position from east to west. For example, a south-facing panel will have an azimuth of zero degrees and an east-facing panel will have a -90 degree azimuth angle. With all solar and collector angles accounted for, the angle of incidence, θ , can be determined by taking the inverse cosine of Eq. (7).

$$\begin{aligned} \cos \theta = & \sin \delta \sin \phi \cos \beta - \sin \delta \cos \phi \sin \beta \cos \gamma \\ & + \cos \delta \cos \phi \cos \beta \cos \omega + \cos \delta \sin \phi \sin \beta \cos \gamma \cos \omega \\ & + \cos \delta \sin \beta \sin \gamma \sin \omega \end{aligned} \quad (7)$$

Equation (7) gives the relationship of the angle of incidence of beam radiation on a tilted surface to all other angles defining the sun and that surface. The angle of incidence of beam radiation on a surface and the solar zenith angle are now defined and the actual quantity of solar radiation on a surface can be determined.

In calculating the total solar radiation on a horizontal surface, the beam and diffuse components typically have to be treated separately and as such, calculated separately. There are several methods available to determine the beam and diffuse components of radiation as seen in Fig. 11, but the method used here is the Erbs et al. correlation of Eq. (8).

$$\frac{I_d}{I} = \begin{cases} 1.0 - 0.09k_T & \text{for } k_T \leq 0.22 \\ 0.9511 - 0.1604k_T + 4.388k_T^2 - 16.638k_T^3 + 12.336k_T^4 & \text{for } 0.22 < k_T \leq 0.80 \\ 0.165 & \text{for } k_T > 0.8 \end{cases} \quad (8)$$

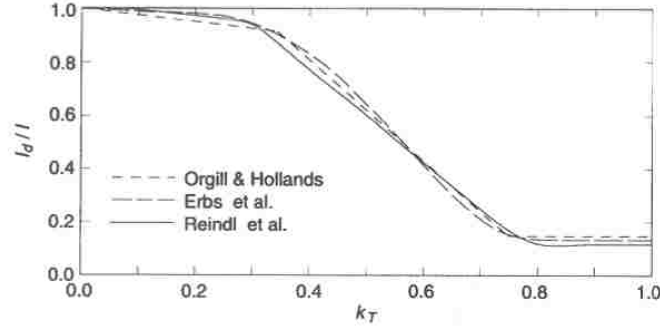


Figure 11. The ratio I_d/I as a function of hourly clearness index k_T showing the Orgill and Hollands (1977), Erbs et al. (1982), and Reindl et. al. (1990a) correlations. [5]

I is the global horizontal irradiance for an hour, I_d is the diffuse horizontal irradiance, and k_T is the hourly clearness index. The clearness index is found from dividing the global horizontal irradiance by the extraterrestrial radiation. Depending on the value of k_T , the diffuse horizontal irradiance I_d can then be determined by multiplying the value of the ratio I_d/I by I . Since the global horizontal irradiance consists of the beam and diffuse components, the beam component can be found simply by subtraction. ($I=I_d+I_b$)

The diffuse horizontal irradiance on a tilted surface, I_{dT} , can then be found by using the collector tilt angle and the diffuse horizontal irradiance within Eq. (9).

$$I_{dT} = I_d \left(\frac{1 + \cos \beta}{2} \right) \quad (9)$$

The beam radiation incident on a tilted surface can be found by multiplying the beam component from the horizontal surface, I_b , by the geometric factor, R_b . The geometric factor is the ratio of the cosine of the angle of incidence from a tilted surface to the cosine of the zenith angle of the sun at that point in time as shown in Eq. (10). Average values of

the geometric factor by month can be found for various latitudes and tilts, such as that shown in Fig. 12 from Duffie and Beckman.

$$R_b = \frac{\cos \theta}{\cos \theta_z} \quad (10)$$

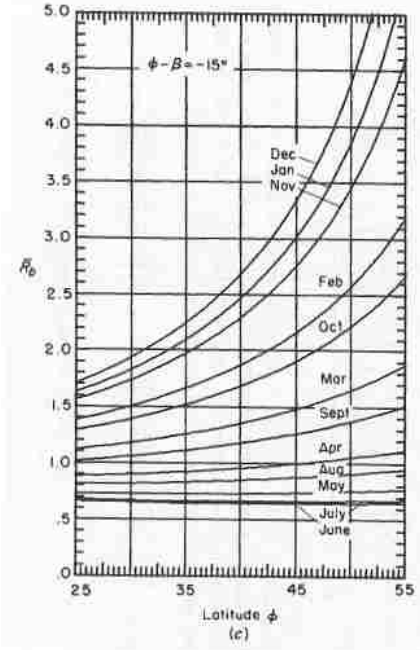


Figure 12. Estimated [average] R_b for surface facing the equator as a function of latitude for various $(\phi - \beta)$, by months. (c) $(\phi - \beta) = -15^\circ$. [5]

The last component needed in determining the total solar radiation on a tilted surface is the radiation that is reflected from the ground onto the collector. The albedo of the surface upon which the collector rests can be used for the ground reflectivity, ρ_g . The reflected component of radiation is then found by

$$I_{gT} = \rho_g I \left(\frac{1 - \cos \beta}{2} \right) \quad (11)$$

Finally, the total solar radiation is found from Eq. (12) by the summation of the beam, diffuse, and ground-reflected radiation components on a tilted surface.

$$I_T = I_b R_b + I_d \left(\frac{1 + \cos \beta}{2} \right) + I \rho_g \left(\frac{1 - \cos \beta}{2} \right) \quad (12)$$

CHAPTER 2

LITERATURE REVIEW

2.1 Solar Thermal History in the United States

The early twentieth century was marked by the discoveries of major oil fields in the United States. These discoveries shadowed the new efficiencies of solar collector concepts from the late eighteenth century, which had just started to improve because of the production of inexpensive, clear glass used as covers. Flat plate collectors for hot water heating became commercially popular between the 1920s and 1940s in California and Florida where the population was loosely spread and natural gas was not yet available. Solar energy research was not financially supported until the 1960s. It was not until the latter 1970s that evacuated tubular collectors were developed by Owens-Illinois and General Electric. [9]

2.2 Previous Analyses

There are many components that go into the design of a solar thermal system, as described in Chapter 1, and each of these components must be examined along with the system as a whole. Consequently, a great deal of information can be gathered in regard to solar thermal systems. The first topic of interest is the solar thermal collector being used in the system, the evacuated tube collector. The next concern is the immersed coil heat exchanger which is responsible for transferring that generated solar energy to a useful source. The storage of that thermal energy is also essential to the solar thermal system so that the energy can be used at a later time for either space heating or domestic water consumption. Space heating from hydronic radiant flooring is another major topic of investigation. Finally, solar thermal system design efforts from the past are studied.

2.2.1 Evacuated Tube Collectors

Evacuated tube collectors are described in their various forms in a recent article by Pluta [10]. Also described are the processes for heat transfer within the tubes and the equations for transmission through the glass cover of the incident solar radiation. The performance of both evacuated tube collectors and flat plate collectors are compared for various incident angles. The incident angle of the sun on a collector has different effects with an evacuated tube collector than with a flat plate collector. Where a flat plate collector is optically symmetrical in all directions of its surface, an evacuated tube collector varies in the transversal and longitudinal planes. Managing this optical non-symmetry has been a challenge for some time. Theunissen and Beckman [11] compare the two collector types in terms of the absorber and transmittance also. They used existing ray tracing work to develop an algorithm for interpolating between the transverse and longitudinal incidence angle modifiers (IAM). Carvalho et al. [12] also presented a general approach to incident angle modifier calculation for different collector types including evacuated tubes and compound parabolic collectors. They discussed the methods currently used for determining the IAM for different collectors and the approximations that can be used when a limited number of IAM are presented. This is the case in the following chapter when the incidence angle modifiers are used from the collector ratings of the Solar Rating and Certification Corporation (SRCC). Carvalho et al. suggests that a linear fit of the transversal IAM may be used but also suggests that more complicated fits may be better suited. Based on this recommendation, a polynomial fit of the transversal IAM is created in the following chapter. They also show the equations that can be used for energy calculations given the hourly absorber irradiance.

They present energy calculations for four different system locations with energy estimation errors of less than 1% using commonly available IAM measured values. With an additional measurement of an IAM in both transversal and longitudinal directions they show energy estimation errors of less than 0.1%.

2.2.2 Immersed Coil Heat Exchangers

Solar thermal systems are classified as either direct circulation if the household water flows through the collector or as indirect circulation if the fluid does not combine with household water [13]. For indirect circulation systems, which includes the system currently being analyzed, a heat exchanger must be used to transfer the heat from the solar fluid to the household fluid. There are several types of heat exchangers that can be used, but the chosen heat exchanger for the current application is the immersed coil heat exchangers which is contained within the tank itself. Not only is an in-tank heat exchanger more convenient, it is also the most effective type of heat exchanger because it is located within the tank and reduces heat losses [14]. Some in-tank heat exchangers have fins on the tube exterior, but it was also proven that a smooth coil performs better than a finned one [15].

Mates [16] developed a computer model to calculate the heat transfer from tubular immersed heat exchangers. Three different models of varying complexity are used within the model. One of the heat exchanger models uses 30 nodes to calculate the steady state heat flow from the entire exchanger. A simpler model uses the exchanger inlet and outlet temperatures to calculate the overall heat transfer coefficient from an average of values. In the third model, a constant effectiveness is given for a set of representative thermal conditions. The effectiveness is then used to find the heat flow for each time step. They

also found that buoyant forces kept the tank fully mixed except during water draws. Properties for changing water temperature were also discussed and the authors found the UA value could change up to 40 percent due to variable water properties [16].

A more recent experimental study was performed by Logie et al. of three different immersed coil heat exchangers to describe the internal and external flows and heat transfers. The study was used to better model the position of the heat exchangers in the thermal storage tanks. The heat exchangers described are typical of the types used by many manufacturers. The methods used to calculate the heat transfer coefficients of the coils are also explained [17]. Another important article from Klett et al. [18] shows the equations used to express the thermal performance of heat exchangers used in solar thermal systems in general. They also discuss some of the erratic temperatures that can be found around immersed coils. Many of the equations that could be used in heat exchanger analysis are in [19], [20] and [21].

2.2.3 Solar Thermal Storage

Jordan and Furbo [22] set up experimental solar thermal storage tanks and studied the temperature gradients in the tanks under varying flow rates of water draws. Stratification was ultimately altered by the amount of the draws and the temperature and location of the water entering the tank.

Kleinbach et al. [23] use a multimode and plug flow method to model the temperature distribution in a solar storage tank. The models are compared to experimental data taken on a system at variable flow rates. When the modeled data was compared to the experimental data, the authors found that the fully mixed tank model significantly under predicts the experimentally measured energy quantities.

The authors found that an increase in the number of nodes in the stratified model better predicts the performance, but two to three nodes worked well in the model [23]. Because of this recommendation, two nodes are used in the current solar thermal system model.

Cruickshank and Harrison use experimental testing and a computer simulation in TRNSYS to model a multi-tank solar thermal storage system for a large multi-family building. An instrumented experimental test apparatus was used to evaluate various configurations and geometries for tank storage. The parameters of the systems used are presented and the authors discuss the findings of previous studies with different system arrangements. Various levels of stratification were monitored and were found to increase the performance of the collectors according to Cruickshank and Harrison. Results of the monitored experiments are shown. Custom TRNSYS models were used to simulate the system using non-linear regression curves to fit experimental data. The simulations were run for a complete solar thermal system at two different locations and the system performance was tested using simulated water draws [24]. Also, Rodriguez-Hidalgo et al. developed a proprietary transient simulation to size the storage tank of a solar thermal system. They discuss the recommended ratios between storage tank volumes and solar collector area found in previous work but found that more work is needed to base the size on the occupancy water draw load [25].

Another interesting investigation is that of the charging time for a solar thermal storage tank, which is the amount of time required to heat the tank to its desired temperature. Poz and Kogan [26] use transfer functions to mathematically model the charging time of solar thermal storage tanks. The purpose of the study is to better size

the systems collectors, tanks, and heat exchangers. From the model, temperatures are derived for the various levels in the storage tanks.

2.2.4 Hydronic Radiant Floor Heating

Hydronic Radiant Flooring is another component in the system which requires significant consideration. A good overall discussion is given by Byung-Cheon [27] including the equations for the fluid, floor, and room temperatures, and the heat transfer coefficients. Schematics and diagrams that explain the heat transfer processes in a room are also shown. Different schemes for controlling room temperature are discussed and examples are given with merits and demerits.

A two-dimensional prediction model for radiant floor systems, given by Laouadi [28], can be integrated into building energy simulation software that only uses a one-dimensional model. The heat transfer within the radiant medium and from the radiant floor tubing to the adjacent floor media is calculated and methods for solving the equations are given. The model is validated using experimental data and the results are presented with a maximum difference of 11%. The reasons for the differences are discussed. The model can be used to better predict the surface temperatures and the boiler thermal capacity requirements.

Finally, the experimental thermal performance of twelve commercially available radiant floor systems and floor types are found by Khanna [29] to better understand the processes and develop better testing mechanisms. The radiant floor systems, building techniques, and materials are well described for the experimental apparatus. Flow rates and water temperatures were varied and thermal performance of the systems were

monitored and documented. Overall heat transfer for the systems are presented for varying flow rates and water temperatures.

2.2.5 Solar Thermal System Analysis

Solar thermal systems are examined frequently and often times are concerned with the thermal stratification of the tank or the performance of the collector and tank storage combination, but the analysis of a system including both hydronic radiant floor heating and evacuated tube solar thermal collectors was very sparsely found.

Buzas [30] presents a model of the solar thermal system where each of the components are independently modeled and the outputs are used for the model inputs of the next component. The author describes each of the modeled components including the solar collector, both an internal immersed heat exchanger and an external heat exchanger, and the storage tank with and without the internal heat exchanger. The simulation models for the components are discussed.

Sharp and Loehrke studied the effects of thermal stratification for thermal storage in residential solar thermal applications. The authors discuss the cases for mixing and stratification in the storage tanks and also discuss different modes for space and water heating, and absorption cooling and the effects on the tank temperatures. Of importance is the discussion that stratification plays in the collector performance and the water heating application. [31]

Most recently, Fontanella et al. [32] use the equation based modeling program Modelica for a case study of a real building solar thermal system. The model is for a roof mounted system on a large energy efficient building, ENERGYbase. The manufacturer's parameters for the system are presented and a description of the system is given. A

mathematical model is developed using the equations for the power consumption of the systems pumps, the heat flow rate, efficiency, and IAM of the collectors, and the heat transfer of the heat exchanger. The model is calibrated using existing system data and data from comparable systems. After calibrating the components of the model, the components were combined to make a complete system.

CHAPTER 3

PREDICTING SYSTEM PERFORMANCE

In this chapter, the solar thermal system will be defined in terms of heat lost from or gained by the tank and under what conditions those heat losses and gains occur. The heat transfer into the tank from the solar loop is found first, using two different approximations. Secondly, the heat lost from the tank to the hydronic radiant floor heating system during the heating season will be discussed. The radiant floor heating system is designed in a third party software and requires detailed consideration compared to other heat transfers in and out of the tank. The other heat transfers affecting the tank are then determined, including the heat lost through the tank walls due to stand-by conduction, and the heat lost from the tank by domestic hot water draws, and additionally their replacement by unheated supply water.

3.1 Solar Thermal Collector Analysis

The ultimate goal in a solar thermal collector analysis is to estimate, as best as possible, the thermal heat output of the collector throughout the year. The Solar Rating and Certification Corporation (SRCC) produces ratings for manufacturers by testing their collectors under a variety of parameters. The collector ratings produced by the SRCC offer two methods for determining the thermal heat output of a collector. The first method uses three different levels of incident solar radiation and provides an approximate, corresponding thermal energy output value, depending on the ambient and inlet water temperatures. If the incident solar radiation on the tilted collector falls between these three levels of radiation, then the thermal output must be interpolated. The

second method is in the form of an efficiency equation, which represents the ratio of thermal energy produced by the collector to the solar radiation incident on the collector. The second method is more accurate than the first method since the efficiency equation for determining the thermal output is nonlinear.

Chapter one developed the detailed methodology for determining the total solar radiation available on a tilted surface on an hourly basis, but using average values of solar radiation for a larger time step, such as a day or month, can greatly simplify the analysis. Average monthly values of total solar radiation on a tilted surface in various cities can be found from the Solar Radiation Data Manual, sometimes referred to as the Redbook, produced by the National Renewable Energy Laboratory (NREL). The approximate Redbook values of solar radiation on a tilted surface can be used with the first method of the SRCC to provide a quick approximation of the amount of thermal energy produced by the collector over a year.

A more accurate representation of the annual thermal energy output is found by using the procedure from the previous chapter for the hourly solar radiation on tilt, along with the second SRCC method. The SRCC also provides a necessary modification for the solar radiation available on tilted evacuated tube collectors, which have a discontinuous surface area unlike flat plate collectors. The efficiency equation is then used to determine the hourly thermal energy output from a tilted evacuated tube collector.

3.1.1 Approximation of Thermal Energy Output

First, the location of the solar thermal system must be found within the Redbook database. Shown below in Fig. 13 is the table of average monthly solar radiation on flat-plate collectors facing south at various tilt angles in Las Vegas, NV. Within the table is

the approximate incident solar radiation for an average day in each month of the year. Only a system location and collector tilt angle is needed to find these approximations.

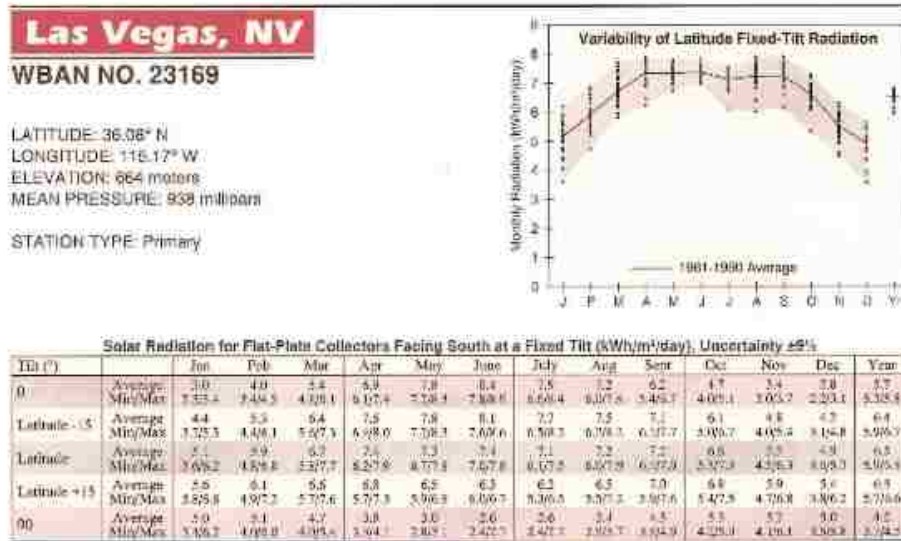


Figure 13. Las Vegas, NV, Solar Radiation for Flat-Plate Collectors Facing South at a Fixed Tilt (kWh/m²/day). [33]

Knowing the approximate incident solar radiation on a collector, the SRCC approach can be used to estimate the corresponding thermal output of the collector with some interpolation. The SRCC certification for a solar thermal collector contains the table of information in Table 1 and will have different values of thermal output for different manufacturers and sized collectors. Across the top of the table are approximate values of the total solar radiation on the surface for days of low, medium and high radiation availability. Along the left side of the table are the temperature conditions that affect the performance of the panel. These temperature conditions indicate that for a given collector inlet water temperature, lower ambient temperatures will reduce the thermal output of the collector.

Table 1. SolarUs, Inc., SL-30 Tubular Collector Thermal Performance Rating in kWh/panel/day. [34]

Kilowatt-hours (thermal) Per Panel Per Day			
Climate \rightarrow	High Radiation (6.3 kWh/m ² /day)	Medium Radiation (4.7 kWh/m ² /day)	Low Radiation (3.1 kWh/m ² /day)
Category ($T_i - T_a$)			
A (8 °C)	14.3	10.8	7.3
B (5 °C)	13.8	10.3	6.8
C (20 °C)	12.3	8.3	5.8
D (60 °C)	10.8	7.1	3.7
E (80 °C)	7.7	4.3	1.3

In order to estimate the thermal output of the collector, the climate category on the far left side must be assumed. The quantity $(T_i - T_a)$ is equal to the difference of the inlet fluid temperature of the collector and the ambient temperature at the system's location. Since the fluid inlet temperature to the collector is not always known, another method for determining the climate category is needed. The SRCC indicates that the climate categories can also be chosen based on the system's application. Category C, for example, corresponds to domestic water heating in a warm climate. As another example, Category D corresponds to space and water heating in a cool climate[34]. If the climate category applications do not match the system being designed, the choice of a category can once again be difficult. An example of this is the system being designed, which has both domestic and space heating applications but for a warm climate instead of a cool climate. The assumption made here in determining the climate category is that during the collector's operation, the inlet water temperature should be very close to the target temperature of the hot water tank. For water heating in Las Vegas, NV, for example, the target water temperature is 48.9 degrees C (120 degrees F). After approximating the value of T_i , the average monthly ambient temperature from the Redbook can be used for the value of T_a . The average $(T_i - T_a)$ for the year in this sample application is therefore around 29.4 degrees C. This average temperature difference could be used to interpolate

values of thermal output between two climate categories, but since this methodology is only an approximation, the closest category, Category C, is chosen in the sample project.

Within the chosen climate category is a relationship between the available solar radiation and the thermal output of the collector. If the relationship is assumed to be linear, then for any solar radiation incident upon the panel, a thermal output can be determined. Continuing with the sample project, the collector tilt angle in Redbook is chosen to be the latitude plus fifteen degrees to take advantage of the lower winter sun for space heating. For each month, the average available solar radiation can be used in the linear relationship to find the thermal output. Figure 14 shows this result for Las Vegas. The high tilt angle in this example reduces the amount of radiation available in the summer when the sun is high in the sky, as illustrated by the dip in the data from June to August.

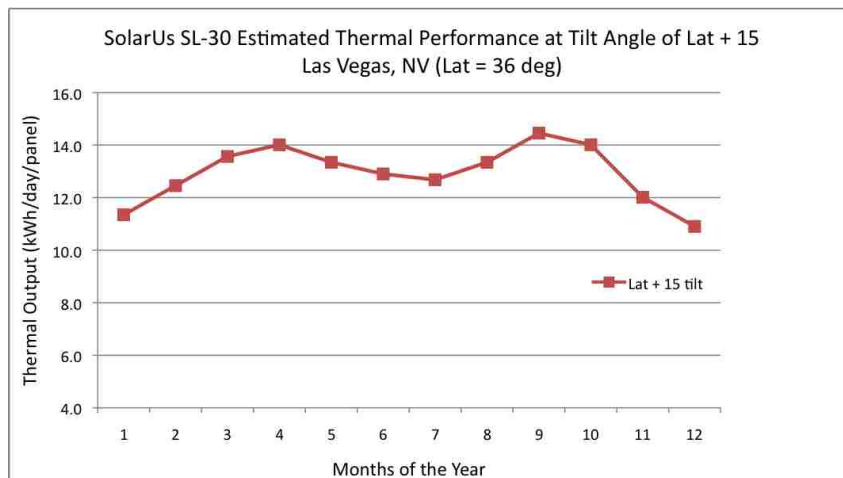


Figure 14. Approximated thermal performance of a SolarUs SL-30 evacuated tube collector tilted at 15 degrees above the latitude for Las Vegas, NV.

A system designer might also want to compare various angles of collector tilt not listed in the Redbook data to determine the best thermal output for their application. A linear interpolation must first be used to determine the available solar radiation at various angles between the Redbook tilt angles. These monthly averages of radiation at new tilt

angles can then be used in the linear relationship to find the collector's thermal output. The result of this approximation for Las Vegas, NV, at tilt angles greater than the latitude is shown in Fig. 15.

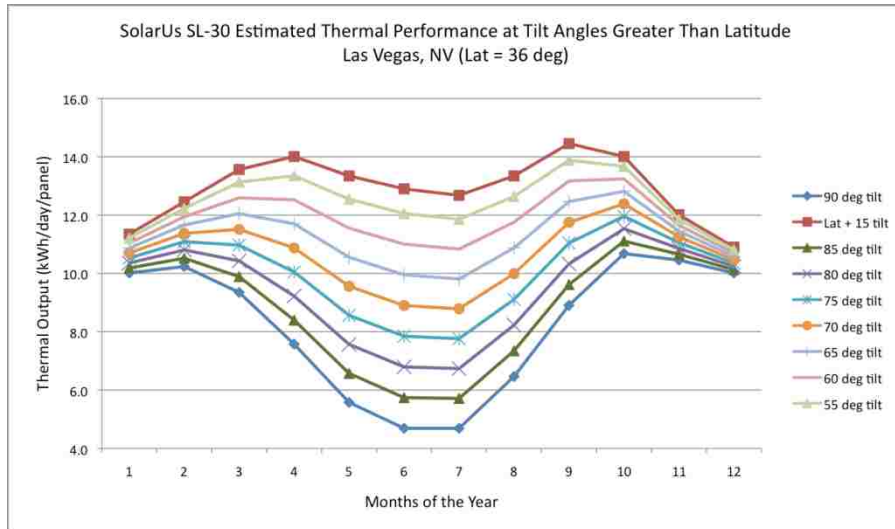


Figure 15. Approximated thermal performance of a SolarUs SL-30 evacuated tube collector tilted at various angles above the latitude for Las Vegas, NV.

The trend in Fig. 15 confirms that with tilt angles closer to vertical, less thermal output is produced in the summer. For this approximated example and the angles shown, the vertical 90 degree tilt shows the lowest summer thermal output and 51 degrees tilt from the horizontal shows the best winter thermal output without losing significant amounts of summer thermal output. A more detailed model than a monthly approximation is needed however, in order to simulate hourly performance of a solar thermal system throughout the year.

3.1.2 Hourly Thermal Energy Output

The sun angle analysis from the previous chapter demonstrated the method for determining the solar radiation incident on a tilted surface. A more accurately estimated thermal output for an evacuated tube collector can now be determined and depends on two specifications from the SRCC. The first specification on the SRCC is the Incidence

Angle Modifier (IAM), which allows the optical properties of an evacuated tube collector to be taken into account in determining the absorbed solar radiation by the collector. The second specification is the efficiency equation which relates the available radiation to the absorbed radiation of the collector. Both the IAM and the efficiency equation coefficients for evacuated tube collectors are unique to the each manufacturer, and are determined during testing and certification by the SRCC.

3.1.2.1 Managing IAM

The cylindrical geometry of the glass covers for evacuated tube collectors are optically nonsymmetrical, meaning that incident sunlight has different components in the transverse and axial planes as shown in Fig. 16.

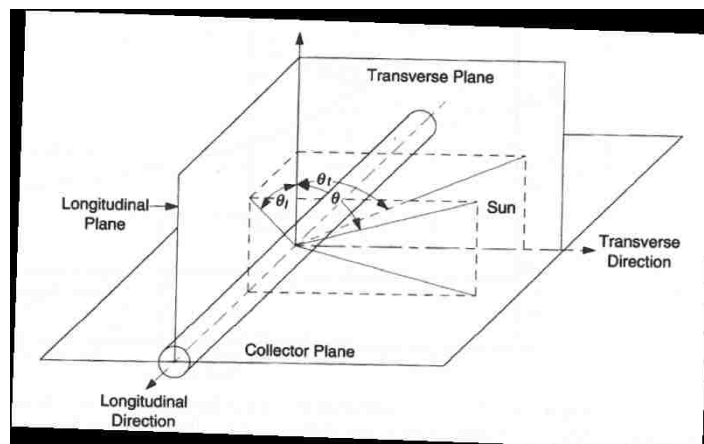


Figure 16. The planes of the evacuated tube incidence angle modifiers. [5]

Normally, the transverse IAM and the longitudinal IAM are multiplied together to get an overall incidence angle modifier according to Pluta [10]. The SRCC provides tested values for the transverse incidence angle modifier at various incidence angles and sometimes also provides tested values for the longitudinal incidence angle modifier as well. In many cases, the longitudinal incidence angle modifier is not given by the SRCC or the manufacturer. The transmittance of the glass cover is also not necessarily provided by the manufacturer, which prevents determination of the longitudinal IAM all together.

This is the case for the sample project using the SolarUs, Inc. SL-30 collector, for which, only the transverse incidence angle modifier is given as shown in Table 2. In this instance, the longitudinal IAM is considered to be unity in order to obtain a value for the overall IAM. In the sample SolarUs collector, a polynomial of the sixth degree is found to best represent the relationship between the transverse IAM and the incidence angle, θ .

Table 2. SolarUs SL-30 transverse incidence angle modifiers. [34]

Transverse Incident Angle Modifier							
θ	10	20	30	45	60	66	70
K_{τ}	1.02	1.07	1.15	1.27	1.39	1.38	0.45

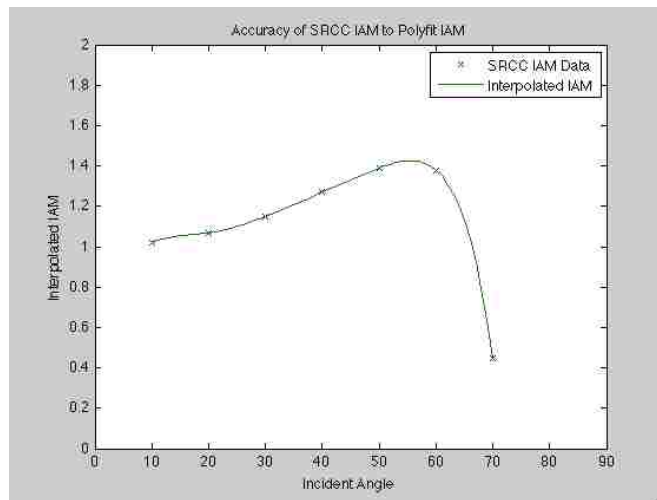


Figure 17. The polynomial fit of the relationship between the IAM and the solar incidence angle.

For any incidence angle throughout the year, an appropriate IAM can be found using the polynomial fit shown in Fig.17. Incidence angles smaller than 10 degrees are set to have an IAM of unity. For incidence angles larger than approximately 70 degrees, the IAM is set to zero which means that the sun is likely to be shining only on the last tube of the collector and no heating is occurring. Equation (12) can now be modified to include the value of the overall incidence angle modifier for any solar incidence angle of an evacuated tube collector. This modification defines what energy travels through the glass

cover to the absorber plate and so, the total incident solar radiation on a tilted surface, I , in Eq. (12) is now S , the total absorbed solar radiation on the collector in Eq. (13) from Duffie and Beckman [5].

$$S = I_b R_b K_{\tau\alpha,b}(\tau\alpha)_n + I_d K_{\tau\alpha,d}(\tau\alpha)_n \left(\frac{1 + \cos\beta}{2} \right) + \rho_g I K_{\tau\alpha,g}(\tau\alpha)_n \left(\frac{1 - \cos\beta}{2} \right) \quad (13)$$

3.1.2.2 Collector Efficiency Equation

The efficiency equation developed from testing a collector during certification is given by the SRCC. The sample efficiency equation from the SolarUs SL-30 collector is shown in Table 3. The variable P is equal to the solar collector inlet temperature minus the solar collector's ambient temperature. The variable G is equivalent to the variable S from Duffie and Beckman and represents the solar radiation absorbed by the collector, which takes into account the affects of the IAMs.

Table 3. SolarUs SL-30 solar thermal efficiency equation.

TECHNICAL INFORMATION	
ISO Efficiency Equation (NOTE: Based on gross area and $(T_i - T_a)$)	
SI UNITS:	$\eta = 0.480 - 1.0520e(P/G) + 0.01100(P/G)^2$
IP UNITS:	$\eta = 0.480 - 0.1601e(P/G) + 0.01100(P/G)^2$

The Greek letter eta, η , represents the ratio of the thermal output of the collector to the radiation absorbed by the collector from Eq. (13). The variable G is equivalent to the S in Eq. (13). The thermal output of the collector, Q_{solar} , in Eq. (14) depends lastly on the gross area of the collector as indicated by the NOTE in the SRCC of Fig. X.

$$Q_{solar} = \eta * (A_{collector} S) \quad (14)$$

3.2 Hydronic Radiant Floor Heating Design

Hydronic radiant floor heating systems are available in a variety of geometries and applications. Often times the tubing for the hot water is laid in the center of the slab-

on-grade concrete floor. Another system geometry applies to joist flooring applications where the tubes are secured to the bottom of the subfloor, between the joists of the flooring structure as shown in Fig. 18. In the case of a joist flooring geometry, a metal heat transfer plate secures the tube in place and promotes evenly distributed heat transfer to the flooring. A major variable in the effectiveness of a radiant floor heating system is the depth of the tubing within the flooring layers. Design modifications can occur during the design of the system in an effort maximize heat transfer for individual applications.



Figure 18. Uponor Joist Trak construction method. [35]

A unique design modification that may be approved by the manufacturer or system installer for joist flooring applications is to mount the tubing and heat transfer plate as close to the finished interior flooring as possible. A hypothetical way to accomplish this improved heat transfer is to use a router to create grooves in the wooden subfloor just beneath the finished flooring. The generated wooden grooves in this instance are made wide enough for the tubing and its surrounding clip diameter, which is how the tube snaps to the heat transfer panel. The detail of the flooring construction is shown in Fig. 19 where the heat transfer panel is indicated as the radiant floor track.

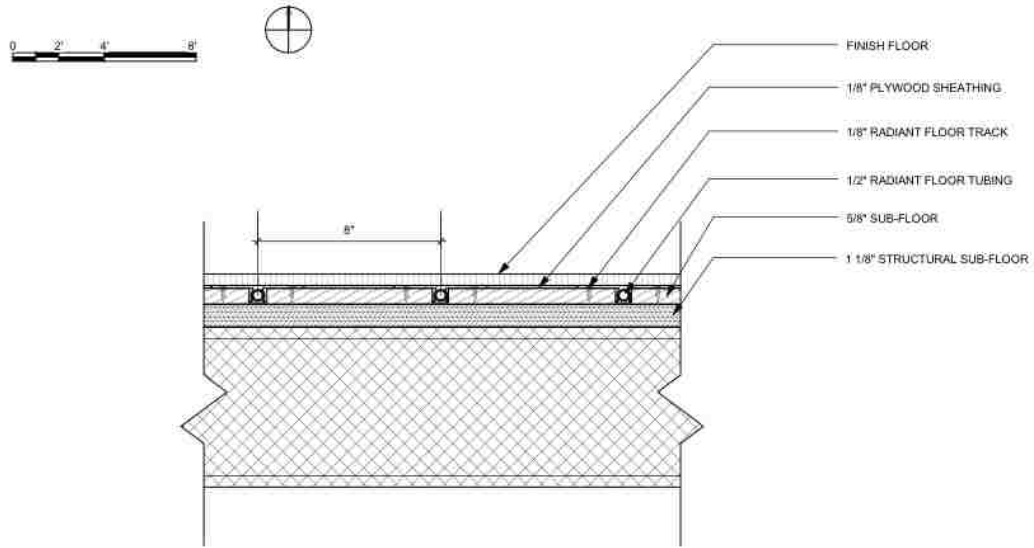


Figure 19. Construction Design Modification of Joist Trak Radiant Flooring. Courtesy of the UNLV 2013 Solar Decathlon Team.

There are also several common tubing layouts for hydronic radiant flooring such as serpentine and counterflow. Some of these layouts and their heat transfer thermal imaging are shown in Fig. 20.

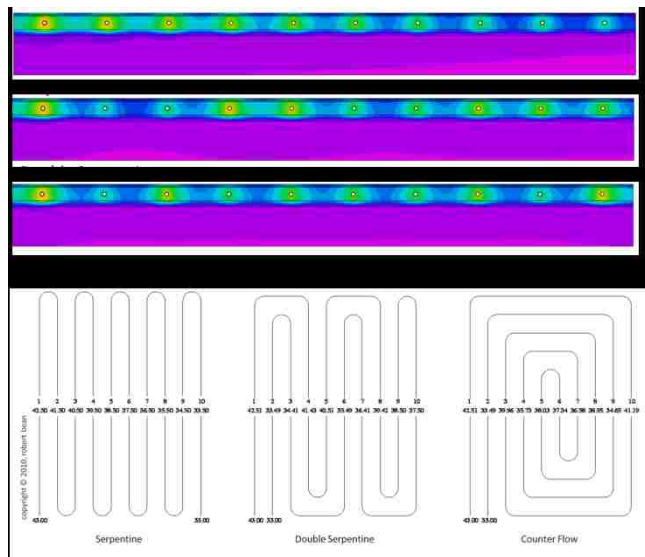


Figure 20. Modeling Radiant Tube Patterns. [36]

The design layout of the tubing may also be modified to promote optimal heat transfer. In the sample layout of Fig. 21, the design path layout is chosen so that the hottest water in

the tubing will first follow the locations of highest thermal infiltration which consist of the outer windows, doors and walls.

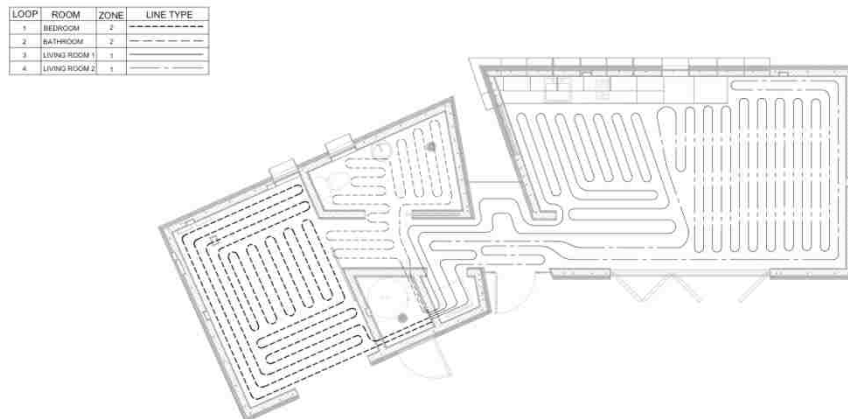


Figure 21. Layout Design Modification of Radiant Floor Tubing. Courtesy of the UNLV 2013 Solar Decathlon Team.

The Advanced Design Suite from Uponor can be used to design the radiant flooring system. Many parameters of a home model go into the design software for a radiant flooring system. Of these parameters are the home's location, the type of flooring system used, the R-value of the walls, flooring and roof, and the setpoint room temperature of the heating system. The design software also requires information about the number of rooms in a home and the dimensions of the rooms, which allows the program to determine a default number of loops, zones and manifolds. To establish a final heat loss value from a home throughout the year, the software requires the locations and dimensions of all the walls, windows and doors in the home. The components and some of the system parameters are shown in the summary of Fig. 22.

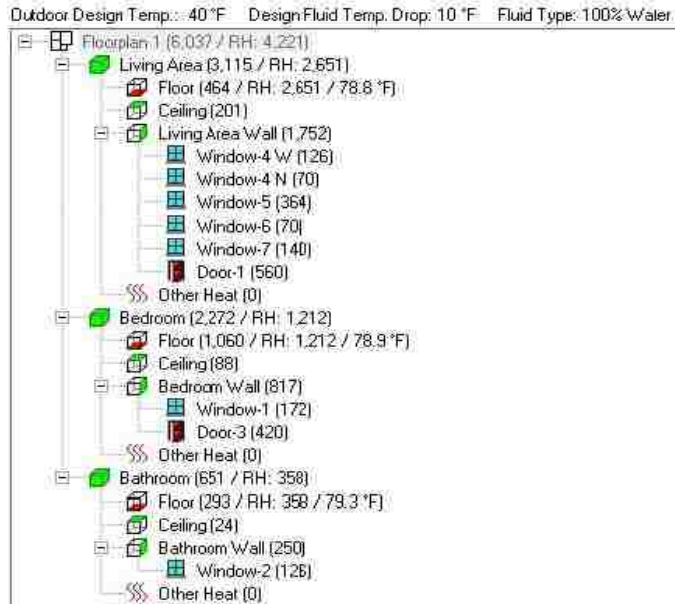


Figure 22. Summary of Home Floorplan Components and Heat Loss. Courtesy of Uponor and the UNLV 2013 Solar Decathlon Team.

Figure 23 gives the results from the radiant flooring design software which contains the parameters of the tubing and the flow rates for all the loops within the system. The second set of software results of Fig. 24 show the total project heat loss along with the volume of the entire radiant flooring system.

Radiant Design Data																
Manifold 1																
Water Temperature:		90.8 °F			Flow Rate:		0.6 USGPM									
Zone Control:		None			Head Loss:		0.6 ft(H ₂ O)									
Control Method:		Tempering Valve			Head Loss S/R:		0 ft(H ₂ O)									
Control Valve Headloss:		0.1 ft(H ₂ O)			S/R Tube Length (One way):		0 ft									
Total Loops:		4			S/R Tube Type:		hePEX 3/4"									
Room	Zone #	Attach Method	Tube Type	Loop #	Area	Unit Heat	Tube Spacing	Leader Length	Loop Length	Flow Rate	Head Loss	Valve Turns	Cover Rv	Surface Temp.	Req. Water Temp.	Design Temp. Drop
Bedroom - Floor	2	Joist Trnk Plates	hePEX 1/2"	1	154	7.9	8	10	251	0.2	0.6	3.73	0.3	78.9	89.8	20
Bathroom - Floor	2	Joist Trnk Plates	hePEX 1/2"	2	42	8.5	8	10	83	0.1	0	1.23	0.3	79.3	90.8	20
Living Area - Floor	1	Joist Trnk Plates	hePEX 1/2"	3	175.3	7.6	8	10	283	0.2	0.3	4.2	0.3	78.8	89	20
Living Area - Floor	1	Joist Trnk Plates	hePEX 1/2"	4	175.3	7.6	8	10	283	0.2	0.3	4.2	0.3	78.8	89	20

Figure 23. System design results from the Uponor Advanced Design Suite for radiant floor design. Courtesy of Uponor.

Project Summary

Project #:	1
Project Name:	UNLV Solar Decathlon 2013
Location:	
Close Date:	
Engineer:	
Design Date Location:	(User-Specified Location)
Outdoor Temperature:	40 °F
Wind Speed:	10 mph
Total Area:	548 ft ²
Construction Quality:	Best
RPH Glycol Level:	100% Water
Design Temp. Drop:	10 °F
Radiant Tubing Volume:	6.3 gallons(US)
Volume Water:	6.3 gallons(US)
Volume Glycol:	0 gallons(US)
Total-Components Load:	3,132 Btu/hr
Total Infiltration Load:	1,088 Btu/hr
Total Floor Downward Load:	1,816 Btu/hr
Total-Radiant Load:	4,221 Btu/hr
Total-Supplemental Load:	0 Btu/hr
Total-Project Heat Loss:	6,037 Btu/hr

Figure 24. Total project heat loss from the Uponor Advanced Design Suite for the radiant floor design. Courtesy of Uponor.

The resulting total project heat loss can be considered the rate of heat that the system is designed to provide. In this way, there is a operational rate for the radiant flooring system. Throughout the heating season, a home will require different quantities of heating in each hour. If the quantity of heat required in each hour is known, then the heat rate provided by the radiant flooring will need to be operational for a portion of that hour. For example, if a home requires 1,500 Btus of heating during some arbitrary hour of the day, the radiant floor system will provide approximately 6,000 Btu/hr for 15 minutes within that hour to meet the heating need. Home energy modeling software such as Energy 10 or EnergyPlus can be used to find a required hourly home energy load throughout the year. Home energy simulations results for heating and cooling often times show frequent cycling between heating and cooling and sometimes produce extreme peaks and valleys in energy needs. Actual heating and cooling differs from these simulations slightly in that the thermostat of a home is usually set to heating or cooling only for several months at a time. One way to resolve both the cycling and extreme values in the results of the energy model, is to first carry an average of several previous heating or cooling values as a basis for comparison. The current energy value being

validated will be compared to the recent average and if it is too much higher than the average, the value will be replaced with the ongoing average. For example, in the simulated performance model, an energy load value in a row will only be kept if the value is less than 150% of the average of the previous 20 load values. This is a simple check to approve each heating or cooling load value and only requires foresight for the first and last 20 hour-values of the year. The sample results of using this energy load filter for the UNLV 2013 Solar Decathlon home energy model are shown in Fig. 25 with the loads before filtering in black and after filtering in red. Positive values are required cooling loads and negative values are required heating loads.

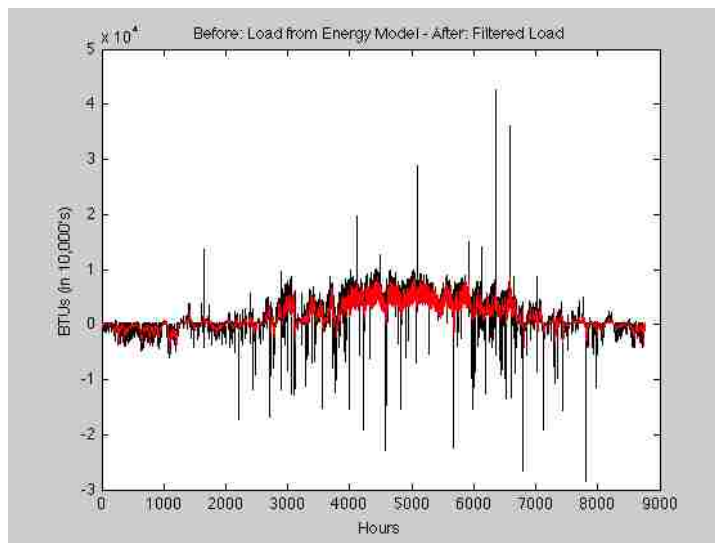


Figure 25. Home heating and cooling energy load values before and after being filtered for abnormalities in values. Original home energy model courtesy of UNLV 2013 Solar Decathlon.

The final consideration in the radiant flooring design is the scenario where heating is required for the home but the hot water storage tank is not hot enough. In this instance, the programmed system simulation records the energy that is not met by radiant flooring so that an auxiliary heating system can be properly sized, such as a mini-split heat pump.

3.3 Tank Analysis

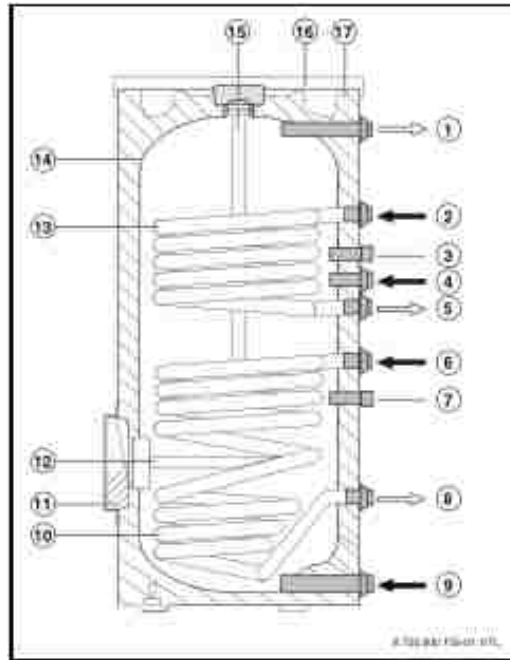


Figure 26. Buderus solar hot water storage tank with dual coil indirect heat exchangers. Tank SM80 or SM100.

The first consideration in the tank analysis is the heat exchanger design. The heat available from the solar collector was determined in the previous chapter and it must now be determined how much of that heat transfers into the tank and what the tank temperature will be after that heat is transferred. The heat exchanger equation of Log Mean Temperature Difference (LMTD) is used to ultimately determine the overall heat transfer coefficient area product, UA , of the coils shown within the tank in Fig. 26. LMTD relates both fluid inlet and outlet temperatures to the efficiency of the coil and the heat that it can transfer. The LMTD equation used for the helical coil heat exchanger in the solar thermal storage tank is given by Eq. (15). A simple counter flow form is used because the bulk water temperature is assumed to be essentially massive. Relating the LMTD back to the quantity of heat being transferred is the overall heat transfer coefficient area product, UA , of Eq. (16).

$$LMTD = \frac{(T_{coilin} - T_{tankout}) - (T_{coilout} - T_{tankin})}{\ln \frac{(T_{coilin} - T_{tankout})}{(T_{coilout} - T_{tankin})}} \quad (15)$$

$$Q_{lowcoil} = UA * LMTD \quad (16)$$

In the programmed simulation of the system, the starting temperature of the tank is the ambient temperature. The coil inlet temperature is determined from equation (17) with the mass flow rate given by the solar collector manufacturer and T_{hot} and T_{cold} corresponding to the inlet and outlet temperatures of the solar collector.

$$Q = \dot{m}c_p (T_{hot} - T_{cold}) \quad (17)$$

The specific heat of water is assumed throughout the tank analysis to be a constant at 50 degrees C. Water is also assumed to be incompressible and the density is also used at 50 degrees C. These constants in the simulated model can be easily changed or made into variables that fluctuate based on average temperatures. In determining UA for example in the simulated model, a tank manufacturer gives a “heat input to the tank rating” in MBtus per hour for both the upper and lower coils. Along with this heat transfer value for the coil, the manufacturer also provides the inlet coil temperature, the before and after tank temperature and the flow rate of the fluid inside the tank and inside the coil. Since Q is already given, Eq. (17) can be used to determine each outlet coil temperature. With all temperatures known for LMTD in Eq. (15), the UA value for the coil can be found from Eq. (16). The overall heat transfer coefficient area product is a property of the heat exchanger itself and once it is determined, it can be used in any further simulation of that coil. The UA is determined for both the upper and lower coil in an 80 and 100 gallon sample solar thermal storage tank. With UA known and using the flow rate within the coil, Eq. (18) can be used to find the outlet coil temperature. [37]

$$\frac{T_{coilin} - T_{coilout}}{T_{coilin} - T_{tankin}} = 1 - \exp\left[\frac{-UA}{\dot{m}c_p}\right] \quad (18)$$

Since the temperatures in and out of the coil are known, the actual amount of heat transferred to the tank can be determined using Eq. (17) again. The heat gained from the solar collector loop heat exchanger is then known.

The heat lost by domestic hot water draws depends on both the hour of the day and the day of the week. For each week of the year, the cycle of seven days of water draws is repeated. If the water in the tank is not as high as the setpoint temperature, the auxiliary water heater provides the makeup thermal energy.

Table 4. Domestic hot water draws over a week. Adapted from competition hot water draws of the 2013 US Solar Decathlon.

Domestic Hot Water Draws (2 gpm, 30 minutes)			
Day	First Draw	Second Draw	Third Draw
1	8:00 AM		
2	8:00 AM	9:00 AM	
3	9:00 AM		
4	2:00 PM	3:00 PM	5:00 PM
5	2:00 PM	3:00 PM	4:00 PM
6	1:00 PM	2:00 PM	3:00 PM
7	8:00 AM	9:00 AM	

These domestic hot water draws represent bathing, doing dishes, or doing laundry throughout the week. As hot water leaves the top of the tank, cold supply water refills the tank from the bottom. The heat lost from the tank because of the hot water draws is equivalent to the hot water flow rate given in Table 4, multiplied by the specific heat of water, and multiplied by the difference between the previous tank temperature and the required setpoint temperature of the tank. The cold water inlet heat transfer will be similar with the difference in temperatures being from the supply water and the previous tank temperature. The final required heat loss quantity is the stand-by loss of the tank and can be determined from the specification by the manufacturer. The value of stand-by loss

could also be determined from Fourier's law of conduction if the thickness and type of insulation on the storage tank are known, along with the average tank fluid temperature and ambient exterior tank temperature.

The overall energy balance for the temperature of the tank can be found from Euler's Integration of Eq. (19).

$$(mC_p)_s \frac{dT_s}{dt} = Q_u - \dot{L}_s \quad (19)$$

After integrating, the time step is clearly shown and hourly data for solar radiation can be used. Ultimately, the new temperature of the tank will be determined from an increase or decrease in the previous hour's temperature.

$$T_s^+ = T_s + \frac{\Delta t}{(mC_p)_s} [Q_u - L_s] \quad (20)$$

This energy balance assumes a fully-mixed tank where the temperature is the same throughout. The value of delta t is chosen to represent a one hour time step based on typical available solar data.

For a stratified tank, each nodal section of the tank will have its own energy balance. In the stratified tank of the simulated model, two nodes are used to represent the temperature difference between the top coil and the bottom coil. The bottom node gains solar energy, loses heat from stand-by losses, gains "heat" from the cold water supply inlet, and also loses heat to the upper node. The heat lost by the lower node is gained in the energy balance of the upper node as warmer fluid shifts upward. The upper node also loses heat because of the domestic water draws, loses heat because of the radiant floor heating system and loses heat due to the stand-by tank loss. In the energy balance for the stratified tank, care must be taken to reduce the mass in the tank to half for each energy

balance equation and also to reduce the outer geometry by half when calculating the stand-by tank loss in each energy balance.

3.4 System Calculations Flow Chart

The overall system flow chart of calculations completed are in Fig. 27.

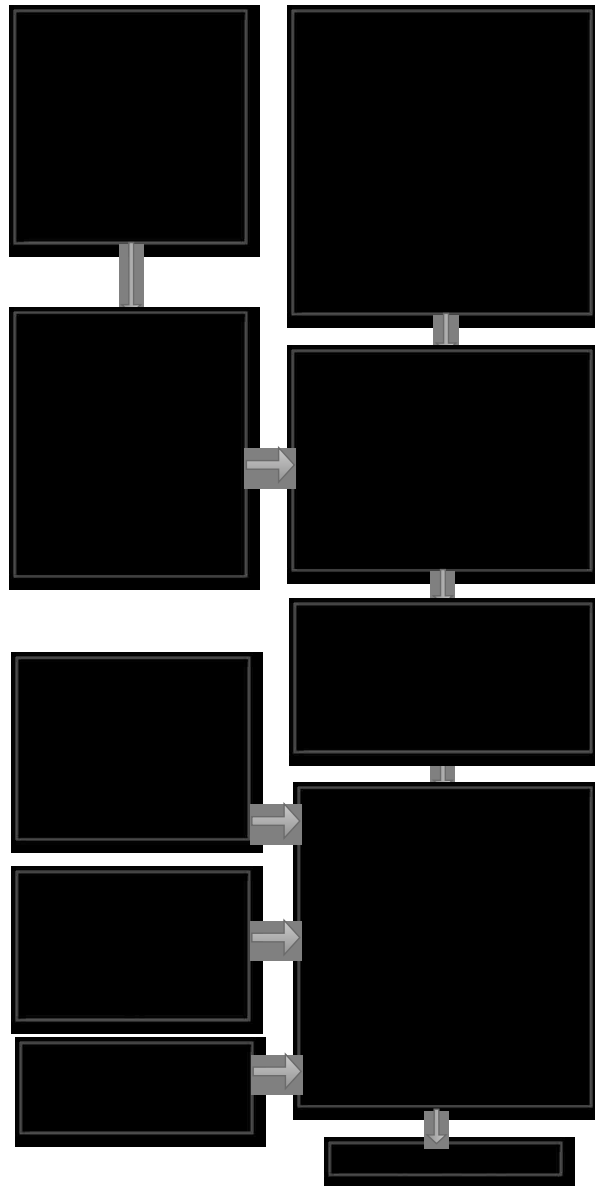


Figure 27. Calculation flow chart for the Solar Thermal System simulation.

CHAPTER 4

EXPERIMENTATION

4.1 Experimental Setup

Two separate experimental setups were used in analyzing the performance of the evacuated tube solar thermal collectors. The first setup tested was the combination of an evacuated tube collector and a storage tank from the same manufacturer. The solar collector consisted of twenty evacuated tubes tilted at 31 degrees. The 40-gallon storage tank allowed for the hot water to flow directly in the top half of the tank, while the cooler water was pumped from the bottom and into the collector manifold. Temperature measurements were taken within the tank and at the fluid inlet and outlet of the collector's manifold. The flow rate of the water through the collector was recorded at 6.87 gallons per minute. Data was collected for three continuous days with this system. The second experiment was conducted at the UNLV Center for Energy Research and included one day of data for a 30-tube SolarUs SL-30 collector tilted at 51 degrees on a sunny day. The components from the two experiments are shown in the following components list and images.

4.1.1 First Experimental Setup



Figure 28. Experiment 1: SEA Evacuated Tube Collector – Set of 18 b) Vacuum tube close-up.

4.1.2 Second Experimental Setup



Figure 29. Experiment 2: SolarUS SL-30 Evacuated Tube Collector.



a) b)
Figure 30. Experiment 2: Pyranometers a) Titled in the plane of the collector b) Resting horizontal.



a) b)
Figure 31. Experiment 2: System components. a) Pump and flow meter in series b) flow meter operating at about 0.7 gallons per minute.



Figure 32. Experiment 2: Datalogging equipment.

Table 5. Experimental Setup Components.

Experimental Setup Components		
Item	Manufacturer	Description
Data Logger, Battery, Power Supply	Campbell Scientific Inc.	CR1000 Data Logger, PS100 Rechargeable Power Supply, 9591 Wall Charger
Pyranometers	Eppley Laboratories	Model PSP Precision Spectral Pyranometer
Thermocouples	Omega Engineering	Type E Thermocouples
Flow Meter	Seametrics	Model SPX-038 Low Flow Meter
Pump	Franklin Electric Co., Inc.	Model TE-3-MD-HC Pump

CHAPTER 5

RESULTS AND DISCUSSION

5.1 First Experimental Results

The results from the first experiment over the three day period show a somewhat cyclic pattern over each day in Fig. 33. Around sunrise each day, the heat transfer to the fluid spikes as the fluid temperature rises significantly from its cool overnight temperature. The same water then continues through the system and eventually back through the collector, where the heat gain to the fluid is less because the fluid is already relatively warm. When the panel outlet temperature is not greater than the tank temperature, the pump shuts off, such as at night where the heat rate is equal to zero in Fig. 33.

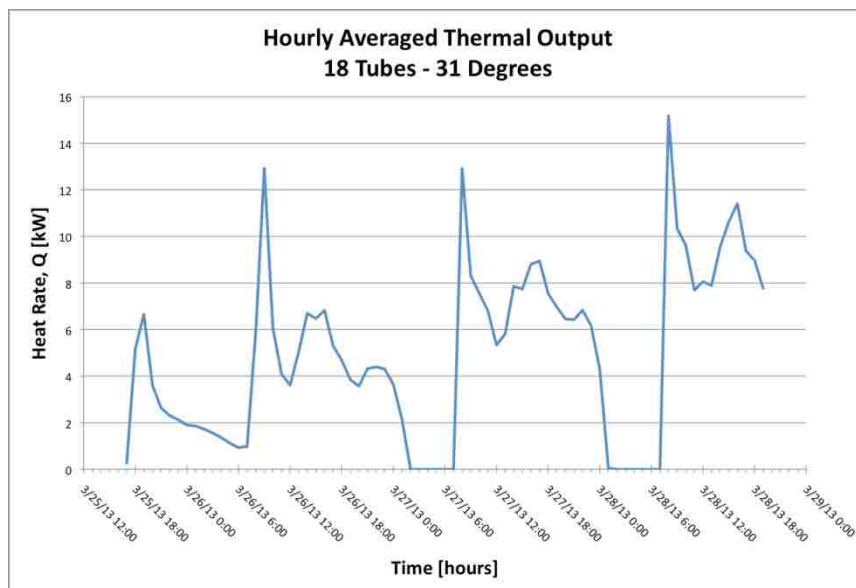


Figure 33. Averaged hourly thermal output from the SEA 18 Tube Collector.

5.2 Second Experimental Results

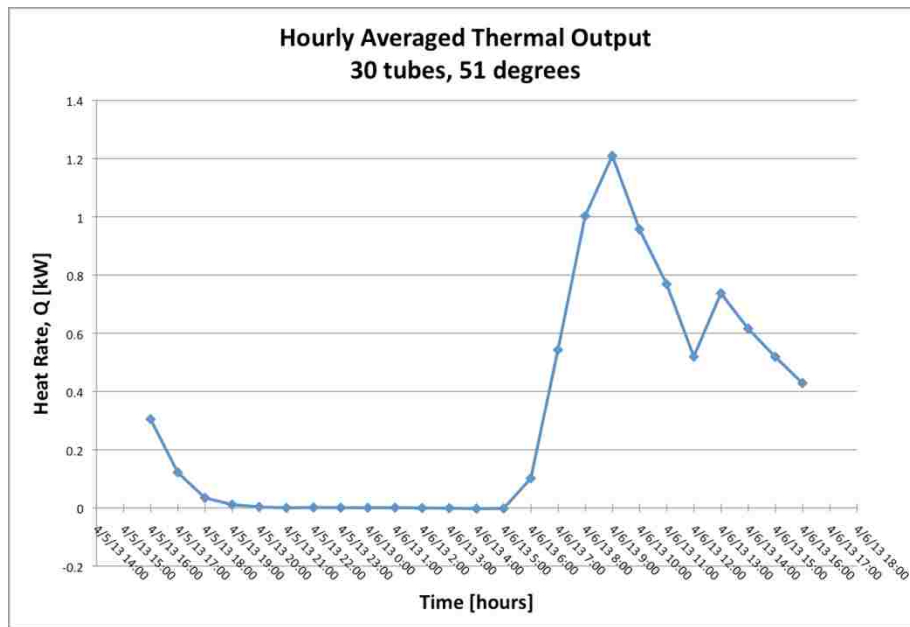


Figure 34. Averaged hourly thermal output from the SolarUs 30 Tube Collector.

A similar pattern is shown in Fig. 34 for experiment 2 during the day of the data collected. The initial start-up temperature spike is present with heat gain to the fluid being less after the collector heat rate reaches an approximate steady state. Because the mass flow rate is two orders of magnitude lower in the second experiment, the rate of heat transfer is much less also, even though the collector is larger.

5.3 Simulation Results

The first simulation performed is for a 100 gallon tank and it assumes that the tank is fully-mixed, or approximately the same temperature throughout. Since the setpoint temperature of the tank is 48.9 degrees Celsius, it is clear from the figure that the tank temperature almost always reaches that temperature goal. The weekly, consistent fluctuations in the tank temperature throughout the year indicate the cycle of hot water

draws from the tank and inlet water supplies to the tank. In the winter, the lower tank temperatures are indicative of the heat loss due to the space heating needs of the home.

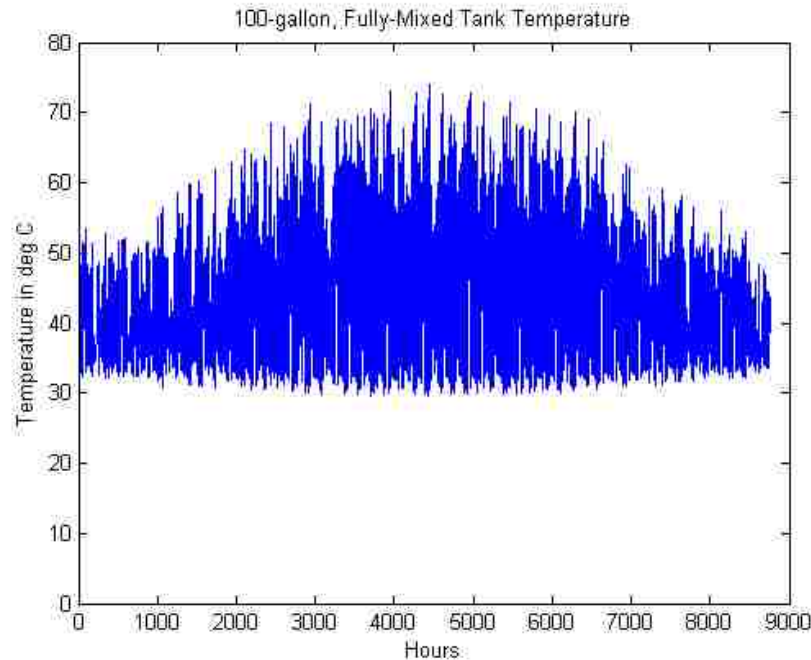


Figure 35. 100 Gallon Fully-Mixed Tank Temperature throughout the year.

When the size of the fully-mixed tank is reduced to the 80 gallon model, the results are shown in Fig. 36. When the volume of the tank is changed in the model, the overall heat transfer coefficient of the coils, the fluid mass, and the stand-by heat loss of the tank also have to be accounted for. The setpoint temperature in this simulation is again reached most of the time throughout the year. The major difference between the 100 and 80 gallon tank is the lower temperatures reached throughout the year in the 80 gallon tank. The smaller tank is affected more than the larger tank by the same hot water draws because the larger volume begins to truly act as a mass storage of heat. The smaller tank also seems to not reach as high of temperatures as the larger tank as frequently.

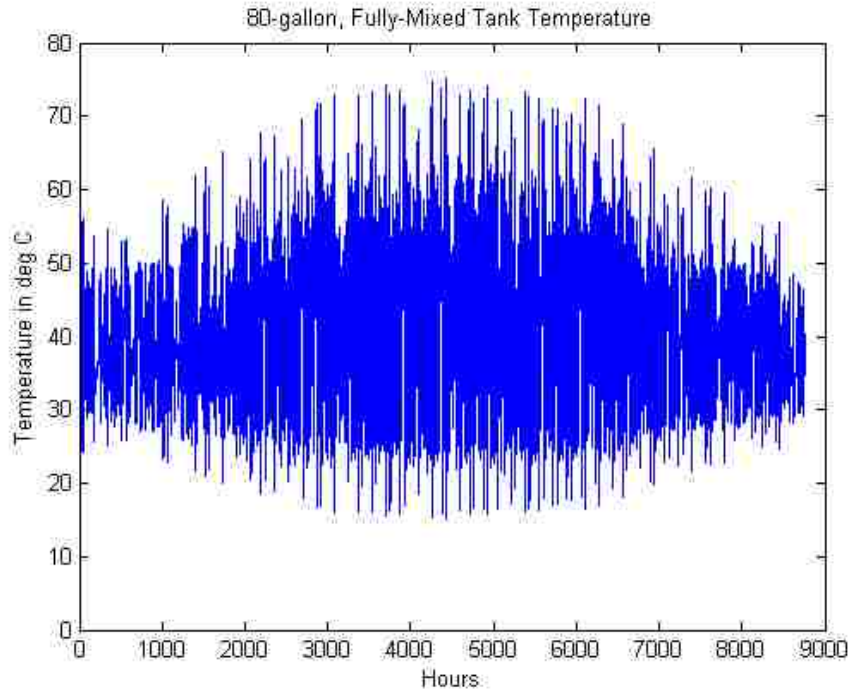


Figure 36. 80 Gallon Fully-Mixed Tank Temperature throughout the year.

With the tank temperatures throughout the year estimated for both the 80 and 100 gallon fully-mixed tanks, an 80 and 100 gallon thermally stratified tank of two nodes is simulated. The result from the 100 gallon stratified tank is shown in Fig. 37. The bottom curve corresponds to the bottom half of the tank hourly temperatures. The curve of the temperature of the top node shows lower tank temperatures in the winter which can again be contributed to the heat loss from space heating. Since the summer months do not have any space heating load for which to pull the heat out of the tank, the temperature rises higher than in the winter.

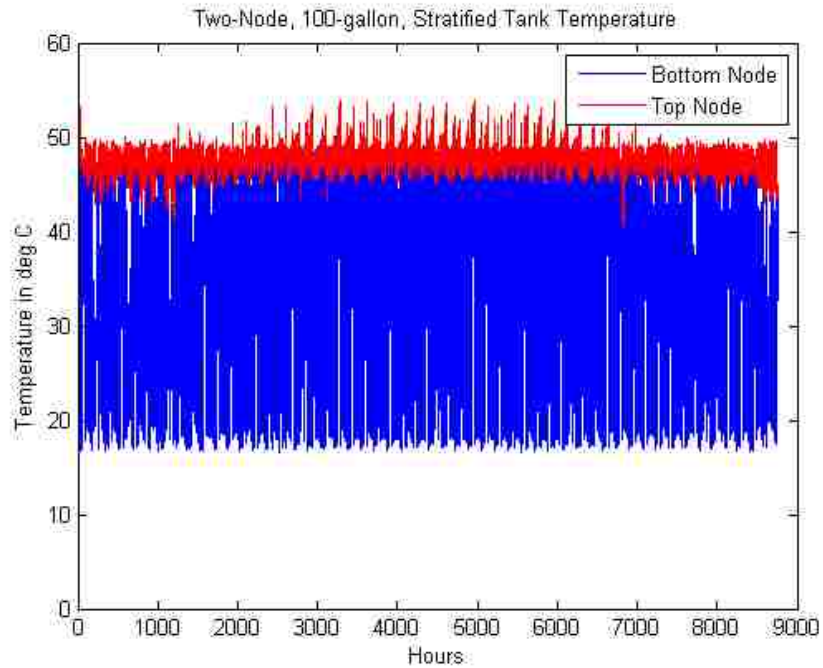


Figure 37. Two Node, 100 Gallon Stratified Tank Temperature throughout the year.

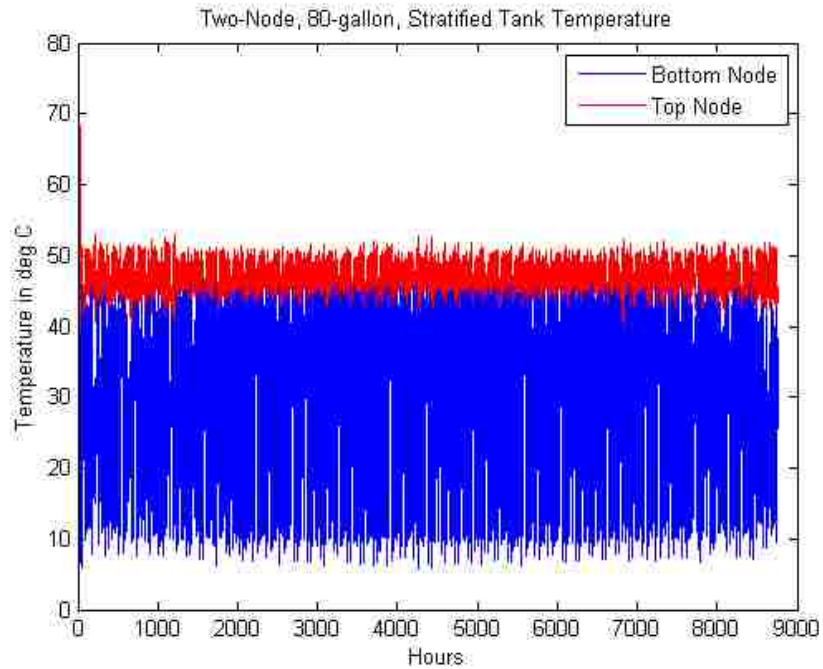


Figure 38. Two Node, 80 Gallon Stratified Tank Temperature throughout the year.

Figure 38 shows the tank temperature results for the two nodes of the 80 gallon stratified tank. The lower temperatures are again seen in the smaller tank indicating a larger affect

by the hot water draws. Since the smaller tank is also less able to store heat, the extra collector thermal energy in the summer is not stored as it is in the 100 gallon tank.

Between the 80 and 100 gallon stratified tanks with two nodes, there seems to be only minor differences in tank temperatures during the year. If the mass of the 80-gallon tank is doubled within the program in an attempt to achieve better storage capabilities, the tank then becomes an approximate model of a stratified, 160-gallon tank as shown in Fig. 39. It can be seen that the temperature of the tank more consistently stays at the setpoint temperature throughout the year than with the smaller tank sizes, which exceed 50 degrees Celsius frequently. The temperatures of the bottom node do not reach as low temperatures as in the smaller tanks which is indicating a minimal affect on the larger volume by the same inlet water draws.

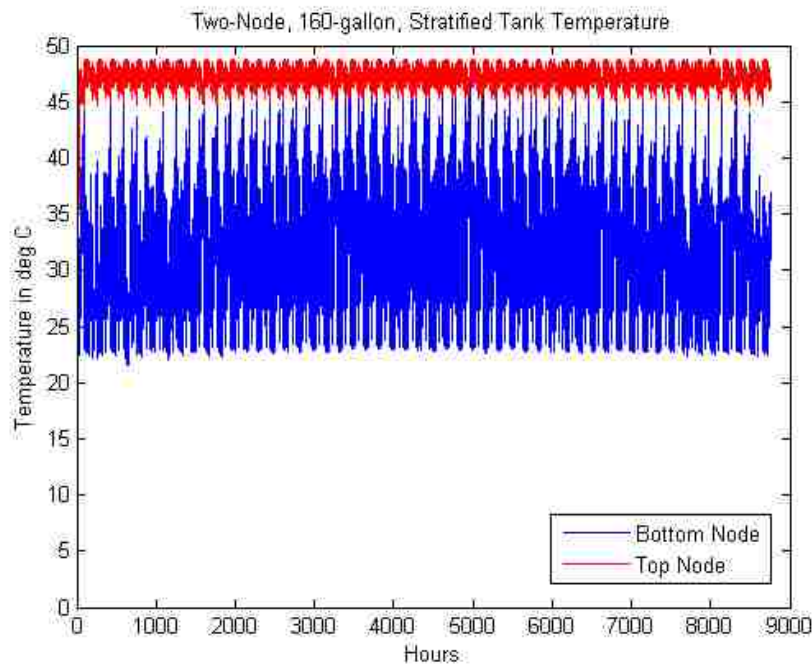


Figure 39. Two Node, 160 Gallon Stratified Tank Temperature throughout the year.

CHAPTER 6

CONCLUSIONS AND RECOMMENDATIONS

6.1 Conclusions

Some conclusions can be drawn regarding the results of the solar thermal system simulations. The temperatures within the tanks fluctuated significantly more with the fully-mixed tank model than with the two-node, stratified tank model. A solar thermal system should be designed carefully if only using a stratified model since high temperatures were only shown in the fully-mixed tank model. On the other hand, if the fully-mixed tank model is used for sizing components, a system designer might undersize the solar collector, which might in turn overheat the system in the case that it behaves as a stratified tank at its end use. Also, the absorbed solar radiation in the simulation is based on the yearly average solar radiation available and might ultimately be more or less. Since a solar thermal system is usually designed to offset the majority of energy needs, and not meet them 100% of the time, it is best to undersize a system and prevent the extra capital cost and system deterioration from occurring at higher operational temperatures. Ultimately, the fully-mixed model and stratified tank model show significant enough differences in results of temperature ranges that both models should be examined when designing a system and average values between the two models will likely yield the best design.

Another conclusion that can be drawn is to choose an approximate tank size that will more often meet the desired setpoint temperature. A range of tank volumes, such as between the 80 gallon and 160 gallon example, should be examined within the model to understand the range of temperatures that the tank can reach and how the energy is

stored. As illustrated in Fig. 37, 38 and 39 of the results, there was an increase in the lowest tank temperatures with increasing tank volume. Therefore, as the tank volume increases, the storage ability of the tank increases also.

6.2 Recommendations

Several improvements could be made to the solar thermal system simulation in the future. The stand-by loss of the tank is placed in the model as a constant, according to the tank manufacturer's specification. Realistically, the heat loss through the walls of the tank will vary depending on the temperature of the water within the tank, the thickness and conductivity of the surrounding tank insulation, and the ambient temperature of the room that contains the tank. If the tank is outdoors, radiation heat transfer could also be significant compared to the convective tank loss. Another improvement to the simulation would be to allow the properties of water to vary with tank and node temperature, rather than holding them constant. It has been shown previously that the overall heat transfer coefficient can change dramatically when the water properties are allowed to fluctuate with temperature [16].

Further investigations within the model are potentially endless. Interesting results have taken shape from dramatically changing the size of the tank in the stratified model. Since doubling the tank size from 80 to 160 gallons in the stratified model affected the temperature of the bottom node, halving the tank size from 80 to 40 gallons might conversely illustrate some overheating in the tank. To fully understand the effect of the nodal analysis on the tank's thermal stratification, using more nodes in the model may also provide more insight. Duffie and Beckman [5] have summarized a significant amount of research in nodal tank analysis and indicate that no more than 10 nodes are

needed to fully understand the thermal stratification potential in most systems. Adding more nodes to the simulation however, is more intensive than varying some other parameters, such as the tilt of the collector. The solar collector in the simulation is tilted to take advantage of the solar energy available in the winter at lower angles of the sun. If the collector in the simulation were tilted to take advantage of the solar energy available in the summer at higher angles of the sun, the results might show high tank temperatures in the summer if the heat gain is not utilized in some alternative way. Also, in order to fully compare the experimental results with the MATLAB simulation, operation of both collectors over the period of a year would be best.

APPENDICES

APPENDIX A NOMENCLATURE

A	area
B	variable for the equation of time
C_p	specific heat capacity [J/kg*C]
E	equation of time [minutes]
I	average hourly available irradiation on a plane [W/m ²]
I_b	direct normal irradiance (DNI) [W/m ²]
I_d	diffuse horizontal irradiance (DHI) [W/m ²]
$K_{\tau\alpha}$	incidence angle modifier (IAM)
L	heat loss [kW or kWh]
L_{loc}	longitude [degrees west of GMT]
LMTD	Log Mean Temperature Difference
L_{st}	standard meridian [degrees]
m	mass [kg]
$m(\dot{m})$	mass flow rate [kg/s]
n	day number of the year (1-365)
Q	heat gain [W, kW or kWh]
R_b	geometric ratio
S	solar irradiance absorbed at a plane [W/m ²]
t	time [seconds]
T	temperature [degrees Celsius, unless indicated otherwise]
UA	overall heat transfer coefficient
β	collector tilt angle from the horizontal [degrees]
δ	declination [degrees]
ϕ	latitude [degrees]
γ	azimuth angle [degrees]
η	efficiency of a solar collector
θ	angle of incidence [degrees]
θ_z	zenith angle [degrees]
ρ_g	albedo or ground reflectivity
ω	hour angle

APPENDIX B MATLAB CODE

```
%%%%%%%%%%%%%%%%%%%%%%%%%%%%%%%%%%%%%%%%%%%%%%%%%%%%%%%%%%%%%%%%%%%%%%%%%%
%%%%%%%%%%%%%%%%%%%%%%%%%%%%%%%%%%%%%%%%%%%%%%%%%%%%%%%%%%%%%%%%%%%%%%%%%%
%%%%%%%%%%%%%%%%%%%%%%%%%%%%%%%%%%%%%%%%%%%%%%%%%%%%%%%%%%%%%%%%%%%%%%%%%%
                SOLAR THERMAL SYSTEM
                SIMULATION BY KIMBERLY HAMMER
                SPRING 2013
%%%%%%%%%%%%%%%%%%%%%%%%%%%%%%%%%%%%%%%%%%%%%%%%%%%%%%%%%%%%%%%%%%%%%%%%%%
                UNIVERSITY OF NEVADA LAS VEGAS
                DEPARTMENT OF MECHANICAL ENGINEERING
%%%%%%%%%%%%%%%%%%%%%%%%%%%%%%%%%%%%%%%%%%%%%%%%%%%%%%%%%%%%%%%%%%%%%%%%%%
%%%%%%%%%%%%%%%%%%%%%%%%%%%%%%%%%%%%%%%%%%%%%%%%%%%%%%%%%%%%%%%%%%%%%%%%%%

% Solar Thermal System components:
%   2 Evacuated Tube Solar Thermal Collectors, 30 tubes each
%   Solar Thermal Storage Tank with dual coil heat exchangers, 100 gal
%   Hydronic Radiant Floor Heating system with 2 zones in 4 loops
%   Direct Domestic Hot Water Draws from tank
%   (Backup Electric On-demand Tankless water heater)
%   (Backup Mini-split heat pump for space heating and cooling)

clear all
clc

rho = 988; % kg/m^3, water density @ 50 deg C, 120 deg F
JperBTU = 1055.0559; % 1055.0559 J = 1 BTU
GalperM3 = 264.172; % 264.172 gallons = 1 m^3

%% LOCATION & TMY3 WEATHER DATA IMPORT (Typical Meteorological Year)

% Choose location for analysis:
% LasVegas (36.083,115.15)-(latitude,longitude)
% SantaAna (33.683,117.867)-(latitude,longitude)
Lat = 36.083; % degrees latitude
Lloc = 115.15; % degrees longitude
Lst = 8*15; % local standard meridian, (Duffie p11), GMT*15

% Only 5 columns from TMY3 needed: ETR, GHI, DNI, DHI and Dry-bulb (C)
% Delete all other columns from TMY3
% Delete all headers and column titles from TMY3
TMY3 = csvread('TMY3LasVegas.csv');
ETR = TMY3(:,1); % W/m^2, extraterrestrial radiation
GHI = TMY3(:,2); % W/m^2, global horizontal irradiance
DNI = TMY3(:,3); % W/m^2, direct normal irradiance
DHI = TMY3(:,4); % W/m^2, diffuse horizontal irradiance
T_amb = TMY3(:,5); % degrees C, ambient temperature

%% GENERATE MONTHS, WEEKS, DAYS AND HOURS

%Creates Month, Day and Hour Vectors
hours = (0:23);
```

```

hour = hours';
day = ones(24,1);
month = ones(24,1);
months = 1;
for j = 1:364;
    for i = 1:24
        hour(j*24+i) = i-1;
        day(j*24+i) = j+1;
        month(j*24+i) = months;
    end
    if j == 30; months = 2; end % (Duffie p14)
    if j == 58; months = 3; end
    if j == 89; months = 4; end
    if j == 119; months = 5; end
    if j == 150; months = 6; end
    if j == 180; months = 7; end
    if j == 211; months = 8; end
    if j == 242; months = 9; end
    if j == 272; months = 10; end
    if j == 303; months = 11; end
    if j == 333; months = 12; end
end

%Creates Week Vector
week0 = day(1:168,1);
week = week0;
for k = 1:52
    week = [week;week0];
end
week = week(1:8760,1);

%% SUN-ANGLE RELATIONSHIPS

% Solar Collector Position Info
beta = 20; % collector slope, degrees from the horizontal (ground)
azi = 0; % collector azimuth, degrees, south = 0, east = -90, west =
+90
refl = 0.18; % reflectivity of ground, assigned a typical albedo value

% Solar Collector Manufacturer Info: SolarUS Tubular Collector, 2*SL-30
eta_o = 0.483; a1 = 1.05630; a2 = 0.0105; % efficiency eq. constants,
SI
A_coll = 4.378; % gross area, m^2, SRCC under 'technical info'
% mdot_test = 0.0207; % kg/s*m^2 from SRCC
% mdot_solar = 0.0429 kg/s given by MFG, used in Efficiency & Energy
Bal.

% Solar Variables Placeholder Matrices
B = ones(8760,1); E = ones(8760,1); decl = ones(8760,1);
Soltime = ones(8760,1); HrAng = ones(8760,1); Clnrns = ones(8760,1);
ZenAng = ones(8760,1); ZenAngdeg = ones(8760,1);
costheta = ones(8760,1); costhetaz = ones(8760,1);
IncAng = ones(8760,1); IncAngdeg = ones(8760,1);

```

```

Rb = ones(8760,1);
r = pi/180; % converting from degrees to radians
DiffFlat = ones(8760,1); DiffTilt = ones(8760,1);
BeamFlat = ones(8760,1); BeamTilt = ones(8760,1);

for i=1:8760
    B(i,1) = (day(i)-1)*(360/365);
    % a variable for equation of time (Duffie p9)
    E(i,1) = 229.2*(0.000075+0.001868*cos(B(i))-0.032077*sin(B(i))-...
        0.014615*cos(2*B(i))-0.04089*sin(2*B(i)));
    % equation of time, E, (Duffie p11)
    decl(i,1) = 23.45*sind(360*(284+day(i))/365);
    % declination of sun, delta, (Duffie p14)
    Soltime(i,1) = hour(i) + ((4*(Lst-Lloc) + E(i))/60);
    % solar time (Duffie p12)
    HrAng(i,1) = -(12-Soltime(i))*15;
    % hour angle (Duffie Ex.1.6.1)

    if ETR(i) == 0;
        Clnrns(i) = 0;
    else Clnrns(i) = GHI(i)/ETR(i); % clearness index, kT, (Duffie p76)
    end

    if GHI(i) < 50; % arbitrary value, W/m^2, filters the weak solar
data
        % collected at sunrise and sunset
        costheta(i,1) = 0;
        costhetaz(i,1) = 0;
    else
        costhetaz(i,1) = cos(Lat*r)*cos(decl(i)*r)*cos(HrAng(i)*r)+...
            sin(Lat*r)*sin(decl(i)*r);
        costheta(i,1) = sin(decl(i)*r)*sin(Lat*r)*cos(beta*r)-...
            sin(decl(i)*r)*cos(Lat*r)*sin(beta*r)*cos(azi*r)+...
            cos(decl(i)*r)*cos(Lat*r)*cos(beta*r)*cos(HrAng(i)*r)+...
            cos(decl(i)*r)*sin(Lat*r)*sin(beta*r)*cos(azi*r)*cos(HrAng(i)*r)+...
            cos(decl(i)*r)*sin(beta*r)*sin(azi*r)*sin(HrAng(i)*r);
    end

    if GHI(i) < 50 || costhetaz(i) <= 0 ;
        Rb(i,1) = 0;
    else
        Rb(i,1) = (costheta(i)/costhetaz(i)); % geometric factor
(Duffie p24)
        if Rb(i) > 3; Rb(i,1) = 3;
        end
        if Rb(i) < 0; Rb(i,1) = 0;
        end
    end % see Duffie, Figure 2.19.1 for monthly Rb averages

    % For Display, Rb value confirmation
    test = [Rb decl month];

    % zenith angle, theta_z, radians, (Duffie p15)
    ZenAng(i,1) = acos(costhetaz(i));
    ZenAngdeg(i,1) = acosd(costhetaz(i)); % zenith angle, degrees

```

```

% angle of incidence, theta, radians, (Duffie p14)
IncAng(i,1) = acos(costheta(i));
IncAngdeg(i,1) = acosd(costheta(i)); % incidence angle, degrees

% beam and diffuse components of global horiz. irradiance using the
% Ers et. al. correlation, see Duffie Figure 2.10.3 & Eq. 2.10.1
if Clnrns(i) > 0.8; DiffFlat(i,1) = GHI(i)*0.165;
elseif Clnrns(i) <= 0.22; DiffFlat(i,1) = GHI(i)*(1 -
0.09*Clnrns(i));
else DiffFlat(i,1) = GHI(i)*(0.9511-0.1604*(Clnrns(i)) +...
4.388*(Clnrns(i)^2)-16.638*(Clnrns(i)^3)+...
12.336*(Clnrns(i)^4));
end
BeamFlat(i,1) = GHI(i) - DiffFlat(i); % Duffie p90, Ex. 2.15.1
DiffTilt(i,1) = DiffFlat(i)*((1+cosd(beta))/2);
BeamTilt(i,1) = BeamFlat(i)*Rb(i);

end

xaxis = 1:8760;
figure(1)
plot(xaxis,DHI)
legend('DHI (measured from TMY3, no solar disk)')

figure(2)
plot(xaxis,DiffFlat)
legend('DiffFlat (from clearness index)')

diffuseplot = DiffFlat-DHI;
figure(3)
plot(xaxis,diffuseplot)
legend('Difference in Diff. Horiz. = DiffFlat(from clearness)-
DHI(TMY3)')

%% SOLAR STORAGE TANK CONSTANTS

% Solar Tank
Cp = 4182; % J/kg*C, specific heat capacity water @ 50 deg C, 120 deg
F
N = 2; % number of nodes in stratified tank, Bottom=1, Top=2
% 100 gallon tank
D = 26.375/39.3701; % tank diameter, convert inch to m
H = 72.25/39.3701; % tank height, convert inch to m
V = 103/264.172052; % tank volume, convert gal to m^3
V_node1 = V/2; V_node2 = V/2;
A_top = pi*(D^2)/4; A_bottom = A_top; A_side = 2*pi*(D/2)*H;
A_tank = A_top + A_bottom + A_side;
A_node1 = A_side/2 + A_bottom; A_node2 = A_side/2 + A_top;
Q_loss = 2200/24; % tank stand-by heat loss in 24 hours, Watts
A_topcoil = 1; % tank top coil surface area, m^2
A_botcoil = 1.8; % tank bottom coil surface area, m^2
V_topcoil = 7; % volume top coil, liters
V_botcoil = 12.1; % volume bottom coil, liters

```



```

% 80 gallon tank
D8 = 26.375/39.3701; % tank diameter, convert inch to m
H8 = 58.875/39.3701; % tank height, convert inch to m
V8 = 79.3/264.172052; % tank volume, convert gal to m^3
V8_node1 = V8/2; V8_node2 = V8/2;
A8_top = pi*(D8^2)/4; A8_bottom = A8_top; A8_side = 2*pi*(D8/2)*H8;
A8_tank = A8_top + A8_bottom + A8_side;
A8_node1 = A8_side/2 + A8_bottom; A8_node2 = A8_side/2 + A8_top;
Q8_loss = 2000/24; % tank stand-by heat loss in 24 hours, Watts
A8_topcoil = 0.9; % tank top coil surface area, m^2
A8_botcoil = 1.3; % tank bottom coil surface area, m^2
V8_topcoil = 6.2; % volume top coil, liters
V8_botcoil = 8.8; % volume bottom coil, liters

%% INCIDENCE ANGLE MODIFIER (Specific to Evacuated Tube Collectors)

% Data from SRCC on the Transverse IAM
ANGLE_data = (10:10:70)';
IAM_data = [1.02;1.07;1.15;1.27;1.39;1.38;0.45]; % SolarUS Tubular SRCC

% IAM Function is created in a polynomial fit, degree 6, from SRCC data
IAM_poly = polyfit(ANGLE_data,IAM_data,6); % finds polyfit
varyangle = 10:1:70;
IAM_interp = polyval(IAM_poly,varyangle); % interpolated IAM values

% Graph compares polyfit IAM function to actual SRCC IAM Data
figure(3)
plot(ANGLE_data,IAM_data,'x',varyangle,IAM_interp,'-')
axis([0 90 0 2])
xlabel('Incident Angle')
ylabel('Interpolated IAM')
legend('SRCC IAM Data','Interpolated IAM')
title('Accuracy of SRCC IAM to Polyfit IAM')

% Placeholder matrix
IAM = ones(8760,1);

% Determines the approximate IAM for hourly Incident Angle
for i=1:8760
    if IncAng(i) > 71.914 % IAM becomes negative at 71.915 degrees!
        IAM(i) = 0;
    elseif IncAng(i) < 10 % IAM is about 1 at low incident angles
        IAM(i) = 1;
    else
        IAM(i) = polyval(IAM_poly,IncAng(i)); % IAM found from polyfit
    end
end

% Figure shows how the IAM and Incident Angle vary throughout the day
% figure(2)

```

```

% time = (1:8760)';
% [x,y1,y2] = plotyy(hour,IncAng,hour,IAM) % plotyy for 2 vertical axes
% xlabel('Hour')
% axes(x(1)); ylabel('Incident Angle (Degrees)')
% axes(x(2)); ylabel('IAM - Incidence Angle Modifier')
% legend('Incident Angle','Interpolated IAM')
% title('How IAM and Incidence Angle Varies Throughout the Day')

%% AVAILABLE SOLAR IRRADIANCE

% Placeholder Matrices
S_BeamTilt = ones(8760,1); S_DiffTilt = ones(8760,1);
S_ReflTilt = ones(8760,1); S_TotalTilt = ones(8760,1);

% Beam, Diffuse and Reflected Components of Solar Insolation
for i=1:8760
S_BeamTilt(i,1) = BeamTilt(i)*IAM(i);
S_DiffTilt(i,1) = DiffTilt(i)*IAM(i);
S_ReflTilt(i,1) = refl*GHI(i)*IAM(i)*((1-cosd(beta))/2);

% Total Solar Insolation on the Tilted Collector
S_TotalTilt(i,1) = S_BeamTilt(i) + S_DiffTilt(i) + S_ReflTilt(i);
% W/m^2, Duffie p299, Eq. 6.17.11
end

% For Display
Solartest = [DiffFlat BeamFlat DiffTilt BeamTilt S_TotalTilt];

%% RADIANT FLOOR SPACE HEATING REQUIREMENTS

% Hourly Heating load pulled in from sample energy-efficient home model
HeatLoad = csvread('HeatLoadLasVegas.csv');
Load = HeatLoad(:,1); % BTUs, the heat load needed every hour of the
year
% negative values are heating requirements, positive values are cooling
AvgLoad = ones(8760,1);
AvgLoad(1,1) = Load(1); AvgLoad(2,1) = Load(2); AvgLoad(3,1) = Load(3);
AvgLoad(4,1) = Load(4); AvgLoad(5,1) = Load(5); AvgLoad(6,1) = Load(6);
AvgLoad(7,1) = Load(7); AvgLoad(8,1) = Load(8); AvgLoad(9,1) = Load(9);
AvgLoad(10,1) = Load(10); AvgLoad(11,1) = Load(11);
AvgLoad(12,1) = Load(12); AvgLoad(13,1) = Load(13);
AvgLoad(14,1) = Load(14); AvgLoad(15,1) = Load(15);
AvgLoad(16,1) = Load(16); AvgLoad(17,1) = Load(17);
AvgLoad(18,1) = Load(18); AvgLoad(19,1) = Load(19);
AvgLoad(20,1) = Load(20);
Heat = ones(8760,1);

for i=1:8760
if i > 8740; AvgLoad(i) = Load(i);
else AvgLoad(i+20,1) = (Load(i)+Load(i+1)+Load(i+2)+Load(i+3)...
```

```

+Load(i+4)+Load(i+5)+Load(i+6)+Load(i+7)+Load(i+8)...
+Load(i+9)+Load(i+10)+Load(i+11)+Load(i+12)+Load(i+13)...
+Load(i+14)+Load(i+15)+Load(i+16)+Load(i+17)+Load(i+18)...
+Load(i+19))/20;
end

if AvgLoad(i) >= 0; % positive average of 3 previous values
    if Load(i) >= 0; % the load is also positive
        if Load(i) > 1.5*AvgLoad(i); Heat(i) = AvgLoad(i);
            % removes positive spikes in cooling demand
        elseif Load(i) < AvgLoad(i)/2; Heat(i) = AvgLoad(i);
            % removes minor values of cooling demand
        else Heat(i) = Load(i);
        end
    end
    if Load(i) <= 0; Heat(i)=AvgLoad(i); % handles heat/cool
cycling
    end
end

    if AvgLoad(i) < 0; % negative average of previous 3 values
        if Load(i) < 0; % the load is also negative
            if abs(Load(i)) > 1.5*abs(AvgLoad(i)); Heat(i)=AvgLoad(i);
                % removes negative plummets in heating demand
            elseif abs(Load(i)) < abs(AvgLoad(i))/2;
Heat(i)=AvgLoad(i);
                % removes minor values of heating demand
            else Heat(i) = Load(i);
            end
        end
        if Load(i) > 0; Heat(i)=AvgLoad(i); % handles heat/cool cycling
        end
    end
end

figure(4)
xaxis = (1:8760);
plot(xaxis,Load,'k',xaxis,Heat,'r')
xlabel('Hours')
ylabel('BTUs (in 10,000's)')
title('Before: Load from Energy Model - After: Filtered Load')

%% EFFICIENCIES OF UPPER AND LOWER TANK COILS, FROM MFG DATA

% Determining U, the overall heat transfer coefficient, of the Upper
and
% Lower Heat Exchangers (coils)
%
% According to the manufacturer, the heat transfer rate from the lower
and
% upper coil were determined experimentally by controlling several
% parameters. The coils were tested separately. Over an hour period,
% the following are know:
%
```

```

% 1) Water temperature flowing into the coil (upper or lower)
% 2) Water temperature flowing into the tank
% 3) Water temperature flowing out of the tank
% 4) Flow rate of water in the boiler coil
% 5) Flow rate of water through the tank
% 6) Surface area of heat exchangers (upper and lower)

% Testing Temperature Conditions
T_coil_in = 80 + 273.15; % convert deg C to Kelvin
T_tank_in = 10 + 273.15;
T_tank_out = 60 + 273.15;

% rho = 972; % kg/m^3, water density @ 80 deg C
% JperBTU = 1055.0559; % 1055.0559 J = 1 BTU
% GalperM3 = 264.172; % 264.172 gallons = 1 m^3

% Same flow rate through upper or lower coil
mdot_solar = 0.7*rho/(60*GalperM3); % gal/min converted to kg/s
(=0.0429)
% mdot_test = 0.0207 kg/(s*ft^2) was used in SRCC testing
(conservative)

% 100 Gallon Tank
% Lower coil calc
mdot100_tank_lower = 209*rho/(3600*GalperM3); % gph convert to
kg/s
Qu100_lower = 157*JperBTU/(3600*1000); % MBtu/hr convert to J/s
A100_lower = 1.8; % m^2
% Upper coil calc
mdot100_tank_upper = 129*rho/(3600*GalperM3);
Qu100_upper = 97.2*JperBTU/(3600*1000);
A100_upper = 1;

% 80 gallon tank
% Lower coil calc
mdot80_tank_lower = 134*rho/(3600*GalperM3);
Qu80_lower = 100.7*JperBTU/(3600*1000);
A80_lower = 1.3;
% Upper coil calc
mdot80_tank_upper = 105*rho/(3600*GalperM3);
Qu80_upper = 78.5*JperBTU/(3600*1000);
A80_upper = 0.9;

% Find outlet coil temperature using various Qus and mdots
T100_lower_out = T_coil_in - (Qu100_lower/Cp*mdot_solar);
T100_upper_out = T_coil_in - (Qu100_upper/Cp*mdot_solar);
T80_lower_out = T_coil_in - (Qu80_lower/Cp*mdot_solar);
T80_upper_out = T_coil_in - (Qu80_upper/Cp*mdot_solar);

%Find LMTD using new coil outlet temperatures
delT = (T_coil_in-T_tank_out);

LMTD100_lower = (delT-(T100_lower_out-T_tank_in))/...
log(delT/(T100_lower_out-T_tank_in));

LMTD100_upper = (delT-(T100_upper_out-T_tank_in))/...
log(delT/(T100_upper_out-T_tank_in));

```

```

LMTD80_lower = (delT-(T80_lower_out-T_tank_in))/...
    log(delT/(T80_lower_out-T_tank_in));

LMTD80_upper = (delT-(T80_upper_out-T_tank_in))/...
    log(delT/(T80_upper_out-T_tank_in));

% Find UA, which equals Qu/LMTD
UA100_lower = Qu100_lower/LMTD100_lower; % in J/s, or W
UA100_upper = Qu100_upper/LMTD100_upper;
UA80_lower = Qu80_lower/LMTD80_lower;
UA80_upper = Qu80_upper/LMTD80_upper;

% Find U, by dividing UA by Area of the upper and lower coils
U100_lower = UA100_lower/A100_lower; % in J/s*m^2, or W/m^2
U100_upper = UA100_upper/A100_upper;
U80_lower = UA80_lower/A80_lower;
U80_upper = UA80_upper/A80_upper;

%% DOMESTIC HOT WATER DRAWS

% At least 1.5 gpm (15 gallons in 10 minutes), round up to 2
% Could be up to 45 gallons or 30 minutes, consecutively
% Avg Water Temp must be >= 110 F

% 1 10/4 8:30am
% 2 10/5 8:30am, 9:30am
% 3 10/6 9:30am
% 4 10/7 2:00pm, 3:30pm, 5:00pm
% 5 10/8 2:30pm, 3:30pm, 4:30pm
% 6 10/9 1:30pm, 2:30pm, 3:30pm
% 7 10/10 8:30am, 9:30am
% 1 10/11 9:30am, switch to 8:30am for computation
% all draws at :30 are rolled back to the hour prior to be conservative

% Placeholder matrices
F = zeros(8760,1); % control function for flow rate of hotin/coldout
water
mdot_hotout = ones(8760,1); % gal/min converted to kg/s
mdot_coldin = ones(8760,1);

for i=1:8760
    % 'week' represents the days of the week (1-7)
    if week(i)==1 && hour(i)==8-1; F(i,1) = 1; end

    if week(i)==2 && hour(i)==8-1; F(i,1) = 1; end
    if week(i)==2 && hour(i)==9-1; F(i,1) = 1; end

    if week(i)==3 && hour(i)==9-1; F(i,1) = 1; end

    if week(i)==4 && hour(i)==14-1; F(i,1) = 1; end
    if week(i)==4 && hour(i)==15-1; F(i,1) = 1; end
    if week(i)==4 && hour(i)==17-1; F(i,1) = 1; end

```

```

    if week(i)==5 && hour(i)==14-1; F(i,1) = 1; end
    if week(i)==5 && hour(i)==15-1; F(i,1) = 1; end
    if week(i)==5 && hour(i)==16-1; F(i,1) = 1; end

    if week(i)==6 && hour(i)==13-1; F(i,1) = 1; end
    if week(i)==6 && hour(i)==14-1; F(i,1) = 1; end
    if week(i)==6 && hour(i)==15-1; F(i,1) = 1; end

    if week(i)==7 && hour(i)==8-1; F(i,1) = 1; end
    if week(i)==7 && hour(i)==9-1; F(i,1) = 1; end

    mdot_hotout(i,1) = F(i)*2*rho/(60*GalperM3); % gal/min convert to
kg/s
    mdot_coldin(i,1) = mdot_hotout(i);

end

%% ENERGY BALANCE ON FULLY-MIXED TANK

% Placeholder Matrices
T_tankold = ones(8760,1);
T_tank = ones(8760,1);
T_panelin = ones(8760,1);
T_panelout = ones(8760,1);
T_paneldel = ones(8760,1);
eta = ones(8760,1); Q_solar = ones(8760,1);
T_botcoilin = ones(8760,1); T_botcoilout = ones(8760,1);
Q_botcoil = ones(8760,1);
Q_topcoil = ones(8760,1);
Q_hotout = zeros(8760,1); Q_elec = ones(8760,1);
Q_coldin = zeros(8760,1);

m = V*rho; % convert gallons to kg, for 100 gallon tank
m8 = V8*rho; % for 80 gallon tank
mdot_floor = 1.2*rho/(60*GalperM3); % gal/min converted to kg/s

% Setting initial values to first step of loop variables
T_tanknew = T_amb(1);
T_botcoilout_new = T_amb(1);
T_setpt = 48.9; % deg C, approximately 120 deg F
T_floorin = (86-32)*5/9; % convert deg F to C
T_floorout = (76-32)*5/9; % convert deg F to C

Q_radiant = mdot_floor*Cp*(T_floorin - T_floorout); % Watts from given
data
T_topcoilout = T_floorout + Q_radiant/(mdot_floor*Cp);

QE_radiant = 6037*JperBTU/3600; % convert Btu/hr to Watts, software's
total
RadiantDiff = 100*(QE_radiant-Q_radiant)/QE_radiant;
% percent diff of radiant Q and the given flow rate w/ delta T

Q_heating = ones(8760,1);
Q_cooling = ones(8760,1);

```

```

% Convert BTUs to Joules and separate heating and cooling loads
time_topcoil = ones(8760,1);

for i=1:8760

    T_tankold(i,1) = T_tanknew; % new tank temperature from i-1 becomes
old

    T_panelin(i,1) = T_botcoilout_new; % panel inlet T = bottom tank
exit T
    T_paneldel(i,1) = T_panelin(i) - T_amb(i); % used in SRCC eff. eq.

    if S_TotalTilt(i) <=0; eta(i,1) = 0;
    else % prevents division by zero, for when the sun is down
eta(i,1) = eta_o - a1*T_paneldel(i)/S_TotalTilt(i) - ...
        a2*((T_paneldel(i))^2)/S_TotalTilt(i);
    end % collector efficiency, Duffie p296, Eq. 6.17.7

    if eta(i,1) <0; eta(i,1) = 0;
    end

    UA80_lower = 7390; % magnitude adjustment to UA
    UA100_lower = 12000; % magnitude adjustment to UA

    Q_solar(i,1) = 2*A_coll*eta(i)*S_TotalTilt(i);
    % Watts, gross area is indicated by SRCC
    T_panelout(i,1) = T_panelin(i) + Q_solar(i)/(mdot_solar*Cp);
    % mdot_solar in kg/s, Cp in J/s*C, T in deg C
    % water temperature exiting the solar collector
    T_botcoilin(i,1) = T_panelout(i);
    % water exiting the collector will be entering the bottom tank coil
    % this neglects the pipe losses during fluid transport to tank
    T_botcoilout(i,1) = T_botcoilin(i) - (T_botcoilin(i) -
T_tankold(i))*...
        (1 - exp(-UA100_lower/(1000*mdot_solar*Cp)));
    % T in deg C, UA in kJ/s, Cp in J/kg*C
    if T_botcoilin(i) > T_tankold(i)
    Q_botcoil(i,1) = mdot_solar*Cp*(T_botcoilin(i) - T_botcoilout(i));
    else Q_botcoil(i,1) = 0; % Q in Watts
    end

    Q_hotout(i,1) = mdot_hotout(i)*Cp*(T_tankold(i)-T_setpt);
    % mdot_hotout has control function for hot water draws
    T_supply = 21; % supply water tank is outdoors, deg C
    Q_coldin(i,1) = mdot_coldin(i)*Cp*(T_supply-T_tankold(i));
    if T_tankold(i) > T_setpt;
        Q_elec(i,1) = 0;
    else Q_elec(i,1) = mdot_hotout(i)*Cp*(T_setpt-T_tankold(i));
    end

    if Heat(i) >= 0;
        Q_cooling(i,1) = Heat(i)*JperBTU; % hourly cool needed, in J
        Q_heating(i,1) = 0;
    else

```

```

        Q_heating(i,1) = -Heat(i)*JperBTU; % hourly heat needed, in J
        Q_cooling(i,1) = 0;
    end
    time_topcoil(i,1) = Q_heating(i)/Q_radiant;

    % Calculates new tank temperature
    % T in degrees C, time in seconds, m in kg, Cp in J/kg*C, Q in
    Watts

    if T_tankold(i) <= T_setpt;
        T_tank(i,1) = T_tankold(i) + (1/(m*Cp))*(Q_botcoil(i)*3600 +...
            Q_coldin(i)*1800 - ...
            Q_hotout(i)*1800 - Q_loss*3600);
    else
        T_tank(i,1) = T_tankold(i) + (1/(m*Cp))*(Q_botcoil(i)*3600 +...
            Q_coldin(i)*1800 - Q_radiant*time_topcoil(i) - ...
            Q_hotout(i)*1800 - Q_loss*3600);
    end
    % values to store for the next iteration
    T_botcoilout_new = T_botcoilout(i);
    T_tanknew = T_tank(i);

end

figure(5)
plot(xaxis,Q_elec/1000)
xlabel('Hours')
ylabel('Electric Energy Need in kW')
title('100-gallon, Fully-Mixed, Electric Water Heating Need')

figure(6)
plot(xaxis,T_tank)
xlabel('Hours')
ylabel('Temperature in deg C')
title('100-gallon, Fully-Mixed Tank Temperature')

figure(7)
plot(xaxis,Q_heating,'r',xaxis,Q_cooling,'b')
xlabel('Hours')
ylabel('Energy Load in BTUs')
title('Heating and Cooling Load for an Energy Efficient Home Model')
legend('Heating','Cooling')

%% %% ENERGY BALANCE ON STRATIFIED TANK
%
% %% Placeholder Matrices
% T_tankold = ones(8760,1);
% T_tank = ones(8760,1);
% T_panelin = ones(8760,1);
% T_panelout = ones(8760,1);
% T_paneldel = ones(8760,1);
% eta = ones(8760,1); Q_solar = ones(8760,1);
% T_botcoilin = ones(8760,1); T_botcoilout = ones(8760,1);
% Q_botcoil = ones(8760,1);

```



```

% Q_topcoil = ones(8760,1);
% Q_hotout = zeros(8760,1); Q_elec = ones(8760,1);
% Q_coldin = zeros(8760,1);
%
% m = V*rho; % convert gallons to kg, for 100 gallon tank
% m_1 = m/2; m_2 = m/2;
% m8 = V8*rho; % for 80 gallon tank
% m8_1 = m8/2; m8_2 = m8/2;
%
% mdot_floor = 1.2*rho/(60*GalperM3); % gal/min converted to kg/s
%
% % Setting initial values to first step of loop variables
% T1_tanknew = T_amb(1);
% T2_tanknew = T_amb(1)+1; % starts T2 just barely higher than T1
% T_botcoilout_new = T_amb(1);
% T_setpt = 48.9; % deg C, approximately 120 deg F
% T_floorin = (86-32)*5/9; % convert deg F to C
% T_floorout = (76-32)*5/9; % convert deg F to C
%
% Q_radiant = mdot_floor*Cp*(T_floorin - T_floorout); % Watts from given
data
% T_topcoilout = T_floorout + Q_radiant/(mdot_floor*Cp);
%
% QE_radiant = 6037*JperBTU/3600; % convert Btu/hr to Watts, software's
total
% RadiantDiff = 100*(QE_radiant-Q_radiant)/QE_radiant;
% % percent diff of radiant Q and the given flow rate w/ delta T
%
% Q_heating = ones(8760,1);
% Q_cooling = ones(8760,1);
% % Convert BTUs to Joules and separate heating and cooling loads
% time_topcoil = ones(8760,1);
%
% T1_tank = ones(8760,1); T1_tankold = ones(8760,1);
% T2_tank = ones(8760,1); T2_tankold = ones(8760,1);
%
% for i=1:8760
%
%     T1_tankold(i,1) = T1_tanknew; % new tank temperature from i-1
becomes old
%     T2_tankold(i,1) = T2_tanknew;
%
%     T_panelin(i,1) = T_botcoilout_new; % panel inlet T = bottom tank
exit T
%     T_paneldel(i,1) = T_panelin(i) - T_amb(i); % used in SRCC eff.
eq.
%
%     if S_TotalTilt(i) <=0; eta(i,1) = 0;
%     else % prevents division by zero, for when the sun is down
%     eta(i,1) = eta_o - a1*T_paneldel(i)/S_TotalTilt(i) - ...
%         a2*((T_paneldel(i))^2)/S_TotalTilt(i);
%     end % collector efficiency, Duffie p296, Eq. 6.17.7
%
%     if eta(i,1) <0; eta(i,1) = 0;
%     end
%     UA80_lower = 7390;
%     UA100_lower = 12000;

```

```

% Q_solar(i,1) = 2*A_coll*eta(i)*S_TotalTilt(i);
% Watts, gross area is indicated by SRCC
% if Q_solar(i,1) <=0;
%     T_panelout(i,1) = T_panelin(i);
% else
%     T_panelout(i,1) = T_panelin(i) + Q_solar(i)/(mdot_solar*Cp);
%     % mdot_solar in kg/s, Cp in J/s*C, T in deg C
% end
% In the case of Stagnation check for high setpoint temperature
% if T_panelin(i,1) >=80;
%     T_panelout(i,1) = T_panelin(i);
% else
%     T_panelout(i,1) = T_panelin(i) + Q_solar(i)/(mdot_solar*Cp);
% end
% water temperature exiting the solar collector
% T_botcoilin(i,1) = T_panelout(i);
% water exiting the collector will be entering the bottom tank
coil
% % this neglects the pipe losses during fluid transport to tank
% T_botcoilout(i,1) = T_botcoilin(i)-(T_botcoilin(i) -
T1_tankold(i))*...
%     (1 - exp(-(UA100_lower/(1000*mdot_solar*Cp))));
%     % T in deg C, UA in kJ/s, Cp in J/kg*C
% Q_botcoil(i,1) = mdot_solar*Cp*(T_botcoilin(i) -
T_botcoilout(i));
%     % Q in Watts
% CoilTest(i,1) = T_botcoilin(i) - T_botcoilout(i);
% PanelTest(i,1) = T_panelout(i) - T_panelin(i);
% Q_hotout(i,1) = mdot_hotout(i)*Cp*(T2_tankold(i)-T_setpt);
% mdot_hotout has control function for hot water draws
% T_supply = 21; %Supply water tank is 70 degrees F
% %T_supply = T_amb(i); % T_amb(i); % supply water tank is
outdoors, deg C
% Q_coldin(i,1) = mdot_coldin(i)*Cp*(T_supply-T1_tankold(i));
% if T2_tankold(i) > T_setpt;
%     Q_elec(i,1) = 0;
% else Q_elec(i,1) = mdot_hotout(i)*Cp*(T_setpt-T2_tankold(i));
% end
%
%
% if Heat(i) >= 0;
%     Q_cooling(i,1) = Heat(i)*JperBTU; % hourly cool needed, in J
%     Q_heating(i,1) = 0;
% else
%     Q_heating(i,1) = -Heat(i)*JperBTU; % hourly heat needed, in J
%     Q_cooling(i,1) = 0;
% end
% time_topcoil(i,1) = Q_heating(i)/Q_radiant;
%
% %
% %     if T1_tanknew < T_amb(i);
% %         Q8_loss = 0;
% %     end
% %     if T2_tankold(i) <=T_setpt;
% %         Q_radiant = 0;
% %     end
%
% %
% % % Calculates new tank temperature

```

```

%      % T in degrees C, time in seconds, m in kg, Cp in J/kg*C, Q in
Watts
%      T1_tank(i,1) = T1_tankold(i) + (1/(m_1*Cp))*(Q_botcoil(i)*3600
+...
%          Q_coldin(i)*1800 - Q_loss*3600/2 +...
%          mdot_coldin(i)*Cp*(T2_tankold(i)-T1_tankold(i)));
%      if T2_tankold(i) <= T_setpt;
%      T2_tank(i,1) = T2_tankold(i) + (1/(m_2*Cp))*...
%          (-mdot_coldin(i)*Cp*(T2_tankold(i)-T1_tankold(i))...
%          - Q_hotout(i)*1800 - Q_loss*3600/2);
%      else
%          T2_tank(i,1) = T2_tankold(i) + (1/(m_2*Cp))*...
%          (-mdot_coldin(i)*Cp*(T2_tankold(i)-T1_tankold(i))...
%          - Q_radiant*time_topcoil(i)- Q_hotout(i)*1800 -
Q_loss*3600/2);
%      end
%      %For the case where the lower node is hotter than the upper node
%      %and bouyancy forces mix the nodes:
%      if T2_tank(i,1) < T1_tank(i,1);
%          T2_tank(i,1)=(T2_tank(i,1)+T1_tank(i,1))/2;
%          T1_tank(i,1)=T2_tank(i,1);
%      end
%
%      % values to store for the next iteration
%      T_botcoilout_new = T_botcoilout(i);
%      T1_tanknew = T1_tank(i);
%      T2_tanknew = T2_tank(i);
% end
%
% figure(3)
% plot(xaxis,Q_elec/1000)
% xlabel('Hours')
% ylabel('Electric Energy Need in kW')
% title('100-Gallon, Stratified Tank, Electric Water Heating Need')
%
% figure(4)
% plot(xaxis,T1_tank,'b',xaxis,T2_tank,'r')
% xlabel('Hours')
% ylabel('Temperature in deg C')
% title('Two-Node, 100-gallon, Stratified Tank Temperature')
% legend('Bottom Node','Top Node')
%
% figure(5)
% plot(xaxis,Q_heating,'r',xaxis,Q_cooling,'b')
% xlabel('Hours')
% ylabel('Energy Load in BTUs')
% title('Heating and Cooling Load for an Energy Efficient Home Model')
% legend('Heating','Cooling')
%

```

APPENDIX C DATALOGGING PROGRAM

```
'CR1000
'Created by Short Cut (2.5)

'Declare Variables and Units
Public Batt_Volt
Public SlrW
Public SlrMJ
Public SlrW_2
Public SlrMJ_2
Public Reftemp
Public Temp_C
Public Temp_C_2
Public Temp_C_3
Public Pulse
Public FlowRate

Units Batt_Volt=Volts
Units SlrW=W/m2
Units SlrMJ=MJ/m2
Units SlrW_2=W/m2
Units SlrMJ_2=MJ/m2
Units Reftemp=Deg C
Units Temp_C=Deg C
Units Temp_C_2=Deg C
Units Temp_C_3=Deg C
Units Pulse=Counts
Units FlowRate=gpm

'Define Data Tables
DataTable(Table1,True,-1)
    DataInterval(0,1,Min,10)
    Average(1,Batt_Volt,FP2,False)
    Average(1,SlrW,FP2,False)
    Totalize(1,SlrMJ,IIEEE4,False)
    Average(1,SlrW_2,FP2,False)
    Totalize(1,SlrMJ_2,IIEEE4,False)
    Average(1,RefTemp,FP2, False)
    Average(1,Temp_C,FP2,False)
    Average(1,Temp_C_2,FP2,False)
    Average(1,Temp_C_3,FP2,False)
    Totalize(1,Pulse,FP2,False)
    Average(1,FlowRate,FP2,False)
    Totalize(1,FlowRate,FP2,False)
EndTable

DataTable(Table2,True,-1)
    DataInterval(0,1440,Min,10)
    Minimum(1,Batt_Volt,FP2,False,False)
EndTable


'Main Program
BeginProg
    Scan(30,Sec,1,0)
        'Default Datalogger Battery Voltage measurement Batt_Volt:
```

```

Battery(Batt_Volt)
PanelTemp (RefTemp,250)
'CM3 Pyranometer measurements SlrMJ and SlrW:
VoltDiff(SlrW,1,mV25,1,True,0,_60Hz,1,0)
If SlrW<0 Then SlrW=0
SlrMJ=SlrW*0.003663
SlrW=SlrW*122.100
'CM3 Pyranometer measurements SlrMJ_2 and SlrW_2:
VoltDiff(SlrW_2,1,mV25,2,True,0,_60Hz,1,0)
If SlrW_2<0 Then SlrW_2=0
SlrMJ_2=SlrW_2*0.003529
SlrW_2=SlrW_2*117.647
'Type E (chromel-constantan) Thermocouple measurements
Temp_C:
TCDiff(Temp_C,1,mV7_5C,3,TypeE,RefTemp,True,0,_60Hz,1,0)
'Type E (chromel-constantan) Thermocouple measurements
Temp_C_2:
TCDiff(Temp_C_2,1,mV7_5C,4,TypeE,RefTemp,True,0,_60Hz,1,0)
'Type E (chromel-constantan) Thermocouple measurements
Temp_C_3:
TCDiff(Temp_C_3,1,mV7_5C,5,TypeE,RefTemp,True,0,_60Hz,1,0)
'Pulse measurement Pulse:
PulseCount(Pulse,1,1,2,0,1,0.0)
FlowRate=Pulse*2/1347
'Call Data Tables and Store Data
CallTable(Table1)
CallTable(Table2)
NextScan
EndProg

```

APPENDIX D COMPONENT SPECIFICATIONS



SUPPLIER:
SolarUs, Inc.
965 West Main Street
Branford, CT 06415 USA
www.solarusmfg.com

CERTIFIED SOLAR COLLECTOR

BRAND: SL-30
MODEL: SE-30
COLLECTOR TYPE: Tubular
CERTIFICATION #: 2010126A
Original Certification: January 21, 2011
Expiration Date: October 21, 2022

The solar collector listed below has been evaluated by the Solar Rating & Certification Corporation® (SRCC™) in accordance with SRCC DG-100, Operating Guidelines and Minimum Standards for Certifying Solar Collectors, and has been certified by the SRCC. This award of certification is subject to all terms and conditions of the Program Agreement and the documents incorporated therein by reference.

COLLECTOR THERMAL PERFORMANCE RATING							
Kilowatt-hours (thermal) Per Panel Per Day				Thousands of Btu Per Panel Per Day			
Climate $(T_i - T_a)$	High Radiation (6.3 kWh/m ² day)	Medium Radiation (4.7 kWh/m ² day)	Low Radiation (3.1 kWh/m ² day)	Climate $(T_i - T_a)$	High Radiation (2000 Btu/ft ² day)	Medium Radiation (1500 Btu/ft ² day)	Low Radiation (1000 Btu/ft ² day)
A (-5 °C)	14.3	10.8	7.3	A (-9 °F)	49.8	36.9	24.8
B (5 °C)	13.8	10.3	6.8	B (9 °F)	47.8	35.1	23.1
C (20 °C)	12.9	9.3	5.8	C (36 °F)	42.9	31.9	19.8
D (50 °C)	10.8	7.1	3.7	D (80 °F)	30.2	24.3	12.5
E (80 °C)	7.7	4.3	1.3	E (144 °F)	23.4	18.5	4.3

A- Pool Heating (Warm Climate) B- Pool Heating (Cool Climate) C- Water Heating (Warm Climate)
D- Space & Water Heating (Cool Climate) E- Commercial Hot Water & Cooling

COLLECTOR SPECIFICATIONS					
Gross Area:	4.379 m ²	47.12 ft ²	Dry Weight:	120 kg	265 lb
Net Aperture Area:	3.057 m ²	32.91 ft ²	Fluid Capacity:	1.7 liter	0.5 gal
Absorber Area:	2.406 m ²	25.92 ft ²	Test Pressure:	1103 kPa	160 psi

TECHNICAL INFORMATION		Tested in accordance with:	
ISO Efficiency Equation (NOTE: Based on gross area and $(T_i - T_a)$)			
SI UNITS:	$\eta = 0.483 - 1.65630(P/F) - 0.01050(P^2/G)$	Y Intercept:	0.483
IP UNITS:	$\eta = 0.483 - 0.16616(P/F) - 0.00102(P^2/G)$	Y Intercept:	0.483
		Slope:	-1.718 W/m ² ·°C
		Slope:	-0.003 Btu/hr·ft ² ·°F

Transverse Incident Angle Modifier								Longitudinal Incident Angle Modifier at 30°:	
θ	10	20	30	40	50	60	70	Test Fluid:	Water
K _{tr}	1.00	0.97	0.95	0.92	0.89	0.86	0.80	Test Mass Flow Rate:	0.0327 kg/m ² ·s (0.524 lb/ft ² ·hr)

REMARKS:

Jean Higgins
Technical Director

Print Date: January, 2013
© Solar Rating & Certification Corporation™
www.solar-rating.org • 400 High Point Drive, Suite 400 • Cocoa, Florida 32926 • (121) 213-6037 • Fax: (121) 821-0810




Figure 40. SolarUs SL-30 SRCC (Page 1)

Configurations	Product Updates									
	Vertical Single Coil Models				Vertical Dual Coil Models				Horizontal Single Coil Models	
	SS2	SS164	SS180	SS190	SSM9	SSM106	LT180	LT200	LT300	
Physical Data										
Tank Capacity gal	31.7	62.8	79.3	103	19.5	100	42	53	79	
Diameter in	23.5	27.5	29.5	29.5	20.5	20.5	20.5	25.5	25.5	
Height in	39.5	66.9	56.5	23.4	59.5	72.6	25.5	25.5	25.5	
Length in	-	-	-	-	-	-	36.6	40.7	27.6	
Connection Heat Exchanger Coil In	3/4	1	1	1	1	1	1	1	1	
Connection DHW Outlet In	3/4	1	1	1	1	1	1	1	1	
Connection Cold Water Inlet In	3/4	1	1	1	1	1	1.5	1.5	1.5	
Connection Pressure Inlet In	3/4	3/4	3/4	3/4	3/4	3/4	3/4	3/4	3/4	
Approx. Dry Weight lbs	180	195	251	255	200	200	200	221	261	
Max. OAW Temperature °F	208	222	221	224	222	228	243	250	252	
Max. DHW Operating Pressure psig	145	145	145	145	145	145	145	145	145	
Standby Heat Loss %/Hr	0.36	0.44	0.44	0.54	0.49	0.54	0.39	0.48	0.36	
Max. Heat Exchanger Coil Water Temperature °F	220	220	220	220	220	220	220	220	220	
Max. Heat Exchanger Coil Pressure psig	230	230	230	230	230	230	230	230	230	
Performance Data**										
Heat Input to Tank MBH	30.9	60.2	100.7	157	100.7	193	101.2	137	107.2	
Continuous Rating of	gal/hr	120	107	134	209	134	125	200	120	
Flow Rate Rating	gal/hr	142	144	130	201	192	180	215	200	
Boiler Water Flow Rate gal/hr	11	9	11	11	11	11	11	11	11	
Coil Pressure Drop - [†] of Head	1	1.6	1.1	0.9	1.1	1.9	0.7	0.9	0.7	

Configuration	Stainless Steel Models			
	SS110-40	SS125-48	SS150-60	SS165-72
Physical Data				
Tank Capacity gal	40	67	85	113.4
Diameter in	20	24	24	28
Height in	55	60	70	68
Length in	-	-	-	-
Connection Heat Exchanger Coil In	1	1	1	1
Connection DHW Outlet In	1	1	1	1
Connection Cold Water Inlet In	1	1	1	1
Connection Pressure Inlet In	1/2	3/4	1/2	3/4
Max. DHW Temperature °F	150			
Max. DHW Operating Pressure psig	100			
Standby Heat Loss %/Hr	0.7	0.8	0.5	0.4
Performance Data				
Heat Input to Tank MBH	118	156	171	210
Continuous Rating of	gal/hr	141	211	265
Flow Rate Rating	gal/hr	208	217	250
Boiler Water Flow Rate gal/hr	19	16	16	18
Coil Pressure Drop - [†] of Head	4.5	5.7	6.1	6.5

* Standby heat loss based at 180°F (82°C) DHW Temperature, 80°F (27°C) Room Temperature
 ** Performance data based at 118°F (48°C) Boiler Supply Temperature, 60°F (16°C) Cold Water Inlet Temperature, 180°F (82°C) DHW Outlet Temperature
 † Performance Data based at 180°F (82°C) Boiler Supply Temperature, 60°F (16°C) Cold Water Inlet Temperature, 180°F (82°C) DHW Outlet Temp.



A Tradition of Excellence

The world leader in heating technologies since 1825, Buderus produced the first low-temperature hydronic heating systems. Today, Buderus products are internationally the global standard in high efficiency, low-temperature hydronic heating. All Buderus products are designed to meet strict safety and environmental regulations.

Buderus boilers are quick and easy to install and will install and perform virtually any boiler hot water heating system. They are designed for easy service and service with appropriate maintenance. Buderus boilers deliver the highest efficiencies throughout the lifespan of operation. Buderus is a member of Bosch Thermotechnology.

4408117-1/2015
 Copyright © 2015 Bosch Thermotechnology Corp.
 All rights reserved. Subject to change without notice.

Figure 41. Buderus Solar Thermal Storage Tank Specifications (Page 4)

REFERENCES

- [1] Scheel, T., 2009, "Solar Choices," Contractor: The Online Resource for Mechanical Contracting, How do you decide between flat plate and evacuated tube collectors when specifying products for a plumbing and heating job?
- [2] U.S. Energy Information Administration, 2010, "Solar Thermal Collector Manufacturing Activities 2009," Washington, D.C.
- [3] Sherwood, L., June 2011, "U.S. Solar Market Trends 2010," Interstate Renewable Energy Council, Latham, New York.
- [4] TRNSYS, 2013, "Pricing and Ordering," 2013 (April 6).
- [5] Duffie, J.A., and Beckman, W.A., 2006, "Solar Engineering of Thermal Processes," 3rd Edition, Wiley, Hoboken, N.J., pp. 908.
- [6] Gothika and Belg4mit, "Seasons1," Wikipedia, 2013 (April 7).
- [7] Robert, N., 2010, "Albedo Examples," Wikipedia, 2013 (April 7).
- [8] Stoffel, T., and Wilcox, S., 2004, "Solar Radiation Measurements," NREL Workshop, 2013 (April 7).
- [9] Lunde, P.J., 1980, "Solar thermal engineering: space heating and hot water systems," Wiley, New York, pp. 612.
- [10] Pluta, Z., 2011, "Evacuated Tubular Or Classical Flat Plate Solar Collectors?" Journal of Power Technologies, 91 (3) pp. 158-164.
- [11] Theunissen, P. H., and Beckman, W. A., 1985, "Solar Transmittance Characteristics of Evacuated Tubular Collectors with Diffuse Back Reflectors," Solar Energy, 35 (4) pp. 311-320.

- [12] Carvalho, M., Horta, P., Mendes, J., 2007, "Incidence angle modifiers: a general approach for energy calculations," ISES Solar World Congress 2007: Solar Energy and Human Settlement, Springer, pp. 608.
- [13] U.S. Department of Energy, 2012, "Solar Water Heaters," 2013 (April, 3).
- [14] Plante, R.H., 1983, "Solar domestic hot water: a practical guide to installation and understanding," Wiley, New York, pp. 332.
- [15] Farrington, R. B., and Bingham, C. E., 1988, "Results from Testing and Modeling Residential Load-side Heat Exchangers," Solar Engineering - 1988, ASME, Denver, CO, USA, pp. 1-10.
- [16] Mates, R. E. Jr., 1987, "Model for an Immersed, Collector Side Heat Exchanger," Master's Thesis.
- [17] Logie, W., Frank, E., Haller, M., 2010, "Investigation of immersed coil heat exchangers in regard to heat transfer and storage stratification," Eurosun 2010.
- [18] Klett, D. E., Goswami, D. Y., and Saad, M. T., 1984, "Thermal Performance of Submerged Coil Heat Exchangers Used in Solar Energy Storage Tanks," Journal of Solar Energy Engineering, Transactions of the ASME, 106 (3) pp. 373-375.
- [19] D'Antoni, M., Ferruzzi, G., and Bettoni, D., Fedrizzi, 2012, "Validation of the numerical model of a turnkey solar combi + system," Energy Procedia, Anonymous Energy Procedia, 30, pp. 551.
- [20] Dahm, J., Bales, C., Lorenz, K., 1998, "Evaluation of Storage Configurations with Internal Heat Exchangers," Solar Energy, 62 (6) pp. 407-417.
- [21] Logie, W., and Frank, E., 2009, "Potential improvement in the design of immersed coil heat exchangers," 29th Biennial Solar World Congress of the International Solar

Energy Society, ISES 2009, October 11, 2009 - October 14, Anonymous International Solar Energy Society, Johannesburg, South africa, 1, pp. 717-726.

[22] Jordan, U., and Furbo, S., 2005, "Thermal stratification in small solar domestic storage tanks caused by draw-offs," ISES Solar World Congress 2003, Elsevier Ltd, 78, pp. 291-300.

[23] Kleinbach, E. M., Beckman, W. A., and Klein, S. A., 1993, "Performance Study of One-Dimensional Models for Stratified Thermal Storage Tanks," *Solar Energy*, 50 (2) pp. 155-166.

[24] Cruickshank, C. A., and Harrison, S. J., 2007, "Comparison of multi-tank and large single tank thermal storages for solar DHW applications," 2007 Energy Sustainability Conference, June 27, 2007 - June 30, American Society of Mechanical Engineers, Long Beach, CA, United States, pp. 767-774.

[25] Rodriguez-Hidalgo, M., Rodriguez-Aumente, P., Lecuona, A., 2012, "Domestic Hot Water Consumption Vs. Solar Thermal Energy Storage: The Optimum Size of the Storage Tank," *Applied Energy*, 97 pp. 897-906.

[26] Poz, M. Y., and Kogan, D. Y., 1986, "Determination of Charging Time for Thermal-Storage Tanks in Solar Heating Systems by Various Mathematical Models," *Applied Solar Energy (English Translation of Geliotekhnika)*, 22 (3) pp. 70-74.

[27] Ahn, B., 2011, Korea, "Radiant Floor Heating System, Developments in Heat Transfer," Dr. Marco Aurelio Dos Santos Bernardes (Ed.), ISBN: 978-953-307-569-3.

[28] Laouadi, A., 2004, "Development of a Radiant Heating and Cooling Model for Building Energy Simulation Software," *Building and Environment*, 39 (4) pp. 421-431.

- [29] Khanna, A., 2006, "Development and Demonstration of a Performance Test Protocol for Radiant Floor Heating Systems".
- [30] Buzas, J., 2009, "Block-Oriented Modeling of Solar Thermal Systems," Ph.D. thesis, Szent István University.
- [31] Sharp, M. K., and Loehrke, R. I., 1979, "Stratified Thermal Storage in Residential Solar Energy Applications," *Journal of Energy*, 3 (2) pp. 106-113.
- [32] Fontanella, G., Basciotti, D., Dubisch, F., 2012, "Calibration and Validation of a Solar Thermal System Model in Modelica," *Building Simulation*, 5 (3) pp. 293.
- [33] National Renewable Energy Laboratory, "Solar Radiation Data Manual for Flat-Plate and Concentrating Collectors," RReDC, 2013 (April 8).
- [34] Anonymous "Solar Rating and Certification Corporation," 2013 (April 8).
- [35] Uponor Inc., "Joist Trak Cut Sheet".
- [36] Bean, R., "Radiant Flooring Image of Heat Transfer," Wikipedia, 2013 (April 9).
- [37] Duffie, J.A., and Beckman, W.A., 1974, "Solar energy thermal processes," Wiley, New York, pp. 386.

VITA

Graduate College
University of Nevada, Las Vegas

Kimberly Hammer

Degree:

Bachelor of Science, Mechanical Engineering, 2010
University of Nevada, Las Vegas

Thesis Title: Predicting the Performance of a Solar Domestic Water Heating System
with Evacuated Tube Collectors and Hydronic Radiant Flooring

Thesis Examination Committee:

Chairperson, Robert Boehm, Ph. D.
Committee Member, Woosoon Yim, Ph. D.
Committee Member, Yitung Chen, Ph. D.
Graduate Faculty Representative, Yahia Baghzouz, Ph. D.